

Recombinant Adeno-Associated Virus-Mediated Delivery of MicroRNA-21-3p Lowers Hypertension

Feng Wang,^{1,3} Qin Fang,^{1,3} Chen Chen,¹ Ling Zhou,¹ Huaping Li,¹ Zhongwei Yin,¹ Yan Wang,¹ Chun Xia Zhao,¹ Xiao Xiao,² and Dao Wen Wang¹

¹Division of Cardiology, Departments of Internal Medicine and Institute of Hypertension, Tongji Hospital, Tongji Medical College, Huazhong University of Science and Technology, Hubei Key Laboratory of Genetics and Molecular Mechanisms of Cardiological Disorders (Huazhong University of Science and Technology), Wuhan 430030, China; ²Division of Molecular Pharmaceutics, University of North Carolina Eshelman School of Pharmacy, Chapel Hill, NC 27599, USA

Hypertension is the most important risk factor for cardiovascular diseases worldwide. However, the underlying molecular mechanisms of hypertension are complex and remain largely elusive. Here, we described a novel, microRNA-dependent therapeutic strategy for hypertension. First, we found that plasma microRNA-21-3p (miR-21-3p) levels were significantly reduced both in hypertensive patients and spontaneously hypertensive rats (SHRs) when compared with normal controls. In a series of experiments to dissect the role of miR-21-3p in hypertension, we showed that intravenous delivery of recombinant adeno-associated virus (rAAV)-mediated miR-21-3p expression induced a persistent attenuation of hypertension, with marked amelioration of target organ damages, including cardiac hypertrophy and fibrosis and artery and kidney fibrosis in SHRs, whereas miR-21-3p tough decoys (TuDs) counteracted the above effects. Computational prediction coupled with biochemical experiments revealed that the miR-21-3p-mediated hypotensive reduction effect was accomplished by regulating phenotypic switch of vascular smooth muscle cells (VSMCs) via suppression of the adrenal α 2B-adrenergic receptor (*ADRA2B*) in arteries. Furthermore, we observed that activation of transcription factor *NF- κ B* and *SRF* significantly increased the expression of miR-21-3p in VSMCs. In summary, our study is the first to identify a novel role and mechanism of miR-21-3p in blood pressure control and provides a possible strategy for hypertension therapy using rAAV-miR-21-3p.

INTRODUCTION

Hypertension, persistent elevation of blood pressure, is a common and multifactorial cardiovascular disease. Approximately one billion people worldwide are affected by hypertension, and their progress is affected by both genetic and environmental factors. The underlying mechanisms of hypertension are complex. Several mechanisms have been implicated in the pathogenesis mechanisms of hypertension, including over-activation of the renin-angiotensin aldosterone system,¹ increased activity of the sympathetic nervous system,^{2,3} oxidative stress,⁴ and vascular remodeling.^{5,6} However, the causes and mechanisms of hypertension are still not fully elucidated. Despite continuous advancement in antihypertensive therapy, blood pressure in a considerable proportion of hyperten-

sive patients fails to be effectively controlled.^{7,8} Therefore, it is necessary to identify novel and powerful treatments for hypertension.

MicroRNAs (miRNAs) are endogenous, small non-coding RNAs that have crucial roles in the regulation of gene expression through binding to the 3' UTR of target mRNA at the post-transcription processing steps.^{9,10} During the past few years, miRNAs have been proven to play important roles in a variety of physiological and pathological processes, such as development, metabolism, cellular differentiation, proliferation, cell death, and stress response.^{11–15} In recent years, the implications of miRNAs in the cardiovascular system have gradually been recognized.^{16–18} Genetic gain- and loss-of-function studies have revealed the prominent roles of miRNAs in various cardiovascular diseases, such as cardiac hypertrophy¹⁹ and fibrosis,^{20,21} heart failure,^{22–24} myocardial infarction,^{25,26} angiogenesis,²⁷ atherosclerosis,²⁸ and pulmonary arterial hypertension.²⁹

Recently, an increasing body of evidence showed that miRNAs are associated with hypertension.³⁰ An ingenious study defined the role of aberrant miR-153 as a contributor to the hypertensive state via targeting of *KCNQ4* in an animal model of hypertension.³¹ miRNA-429 has been reported to reduce blood pressure in Sprague-Dawley rats.³² In an early study of cardiac hypertrophy, we found that overexpression of miR-21-3p markedly ameliorated hypertrophic response in cardiomyocytes on the condition of high pressure load induced by transverse aortic constriction in mice.³³ It is well known that miR-21-5p (a guide strand) and miR-21-3p (a passenger strand) are generated from the 5' and 3' arms of the pre-miR-21 precursor, respectively. Recent reports have indicated that miRNA-5p and -3p species often co-express and both are functional.^{34–36} In our previous study, we determined that

Received 6 March 2017; accepted 20 November 2017;
<https://doi.org/10.1016/j.omtn.2017.11.007>.

³These authors contributed equally to this work.

Correspondence: Dao Wen Wang, MD, PhD, Division of Cardiology, Departments of Internal Medicine, Tongji Hospital, Tongji Medical College, Huazhong University of Science and Technology, 1095 Jiefang Ave., Wuhan 430030, China.
E-mail: dwwang@tjh.tjmu.edu.cn



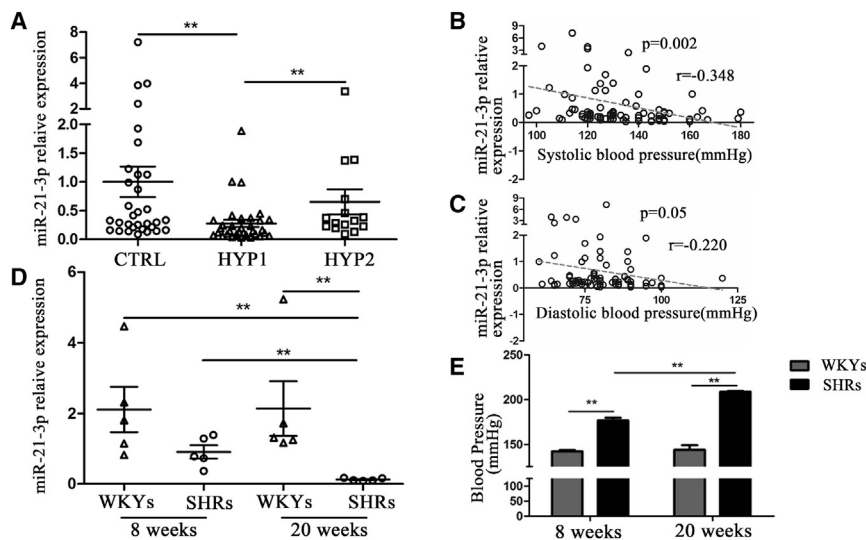


Figure 1. The Expression Patterns of Circulating miR-21-3p in Patients with Hypertension and Spontaneously Hypertensive Rats

(A) The levels of circulating miR-21-3p in hypertension patients. (B and C) The correlation between circulating miR-21-3p levels and blood pressure (B) or diastolic blood pressure (C). (D) The expression of circulating miR-21-3p in WKYs and SHRs. (E) The levels of systolic pressure in WKYs and SHRs. CTRL, health control; HYP1, resistant hypertension group; HYP2, hypertension group with good response to antihypertensive therapy. Data are presented as mean \pm SEM ($n \geq 3$); * $p < 0.05$; ** $p < 0.01$.

rAAV-mediated delivery of miR-21-5p significantly reduced blood pressure and attenuated cardiac hypertrophy in hypertensive rats, and this anti-hypertensive effect was attributed to miR-21-5p-mediated positive modulation of mt-Cytb translation in mitochondria.³⁷ However, the role of miR-21-3p in hypertension is still undefined. In the present study, therefore, our aim was to investigate the roles of miR-21-3p in blood pressure regulation.

RESULTS

Expression Patterns of Circulating miR-21-3p in Hypertension Patients and Spontaneously Hypertensive Rats

Forty-eight patients with hypertension, including 33 patients with resistant hypertension according to response to anti-hypertensive therapy and 15 with a good response to therapy, and 32 healthy volunteers were enrolled in the present study. The clinical characteristics are summarized in Table S1. There were no significant differences in age, sex, fasting glucose, BMI, and other biochemical parameters between hypertension patients and healthy volunteers. The results showed that hypertensive patients have a significantly lower level of circulating miR-21-3p than healthy controls. Interestingly, the patients with resistant hypertension have a lower miR-21-3p level than the patients with a good response to therapy (Figure 1A). Furthermore, results of a correlation analysis showed that the plasma levels of miR-21-3p were negatively correlated with the levels of either systolic or diastolic blood pressure (Figures 1B and 1C).

The level of circulating miR-21-3p was also examined in both spontaneously hypertensive rats (SHRs) and Wistar-Kyoto rats (WKYs) at two different ages (8 weeks old and 20 weeks old), respectively. There was no significant difference in miR-21-3p levels between 8-week-old WKYs and 20-week-old WKYs (Figure 1D), suggesting that the expression of miR-21-3p was not affected by age. Nonetheless, our results showed that plasma miR-21-3p level was significantly lower in SHRs than in WKYs,

and that the plasma miR-21-3p level was remarkably decreased in SHRs at 20 weeks compared with 8 weeks (Figure 1D). In addition, systolic blood pressure of SHRs was also much higher at 20 weeks than at 8 weeks (Figure 1E). Together, these results implied that the concentration of plasma miR-21-3p might be associated with the level of blood pressure *in vivo*.

miR-21-3p Regulates Blood Pressure and the Functions of Arteries in Hypertension

In order to investigate the role of miR-21-3p in hypertension, recombinant adeno-associated virus vectors (rAAVs) were constructed for mediating gain- and loss-of-function of miR-21-3p in a hypertensive animal model. The details of the synthetic sequences are summarized in Table S2. We investigated the impact of different rAAVs vectors on miR-21-3p expression *in vitro* in cell culture. The results showed that pAAV-D(+)-miR-21-3p transfection significantly increased the expression of miR-21-3p, whereas pAAV-D(+)-miR-21-3p-TuDs transfection remarkably reduced the miR-21-3p level (Figure 2A).

Forty-eight 8-week-old male SHRs (180–220 g) were randomly allocated to several groups and respectively received saline, rAAV-GFP, rAAV-miR-21-3p, rAAV-miR-21-3p TuDs, and rAAV-mut-miR-21-3p (about 5×10^{11} viron particles) via intravenous injection. A subgroup of SHRs first treated with rAAV-miR-21-3p was further injected with rAAV-miR-21-3p-TuDs at 14 weeks to reverse the effect of miR-21-3p in hypertension. Six WKYs with the same age were injected with saline as normal control. We noted that systolic blood pressure of SHRs not treated with rAAV-miR-21-3p kept increasing from a baseline of ~ 170 mmHg (at 8 weeks) to a peak of ~ 210 mmHg (at 14 weeks) and remained at a high level, whereas the blood pressure of control WKYs was always maintained at a normal level of ~ 140 mmHg. However, rAAV-miR-21-3p treatment significantly prevented elevation in the blood pressure of SHRs and the hypotensive effect was maintained stable until the end of the experiment at 30 weeks, whereas rAAV-mut-miR-21-3p did not affect blood pressure (Figure 2B). Interestingly, delivery of rAAV-miR-21-3p TuDs into SHRs treated with rAAV-miR-21-3p at 14 weeks fully reversed the anti-hypertensive effects of miR-21-3p *in vivo* (Figure 2B). These

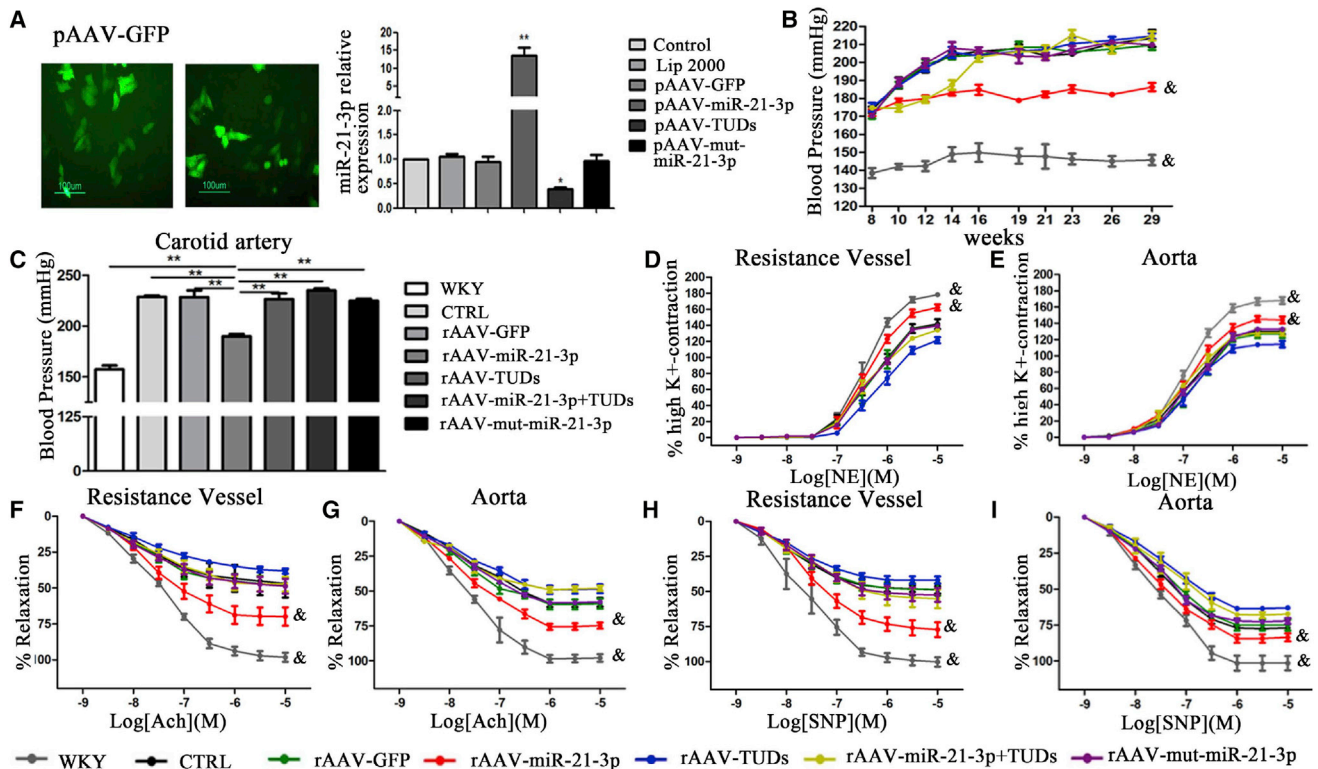


Figure 2. Influence of miR-21-3p on Regulating Blood Pressure and Vascular Function in SHRs

(A) The expressions of miR-21-3p in HUVEC after being administered with various virus-expressing vectors. (B) The levels of systolic pressure in experimental rats. (C) Blood pressure of the carotid artery monitored by the Millar Pressure-Volume System. (D and E) The constrictions induced by NE in the resistance vessel (D) and aorta (E). (F and G) The endothelium-dependent relaxations induced by Ach in the resistance vessel (F) and aorta (G). (H and I) The endothelium-independent relaxations induced by SNP in the resistance vessel (H) and aorta (I). CTRL, SHR-Control (treated with saline). Data are presented as mean \pm SEM ($n \geq 3$); * $p < 0.05$; ** $p < 0.01$; and $^{\&}p < 0.05$ versus SHR control.

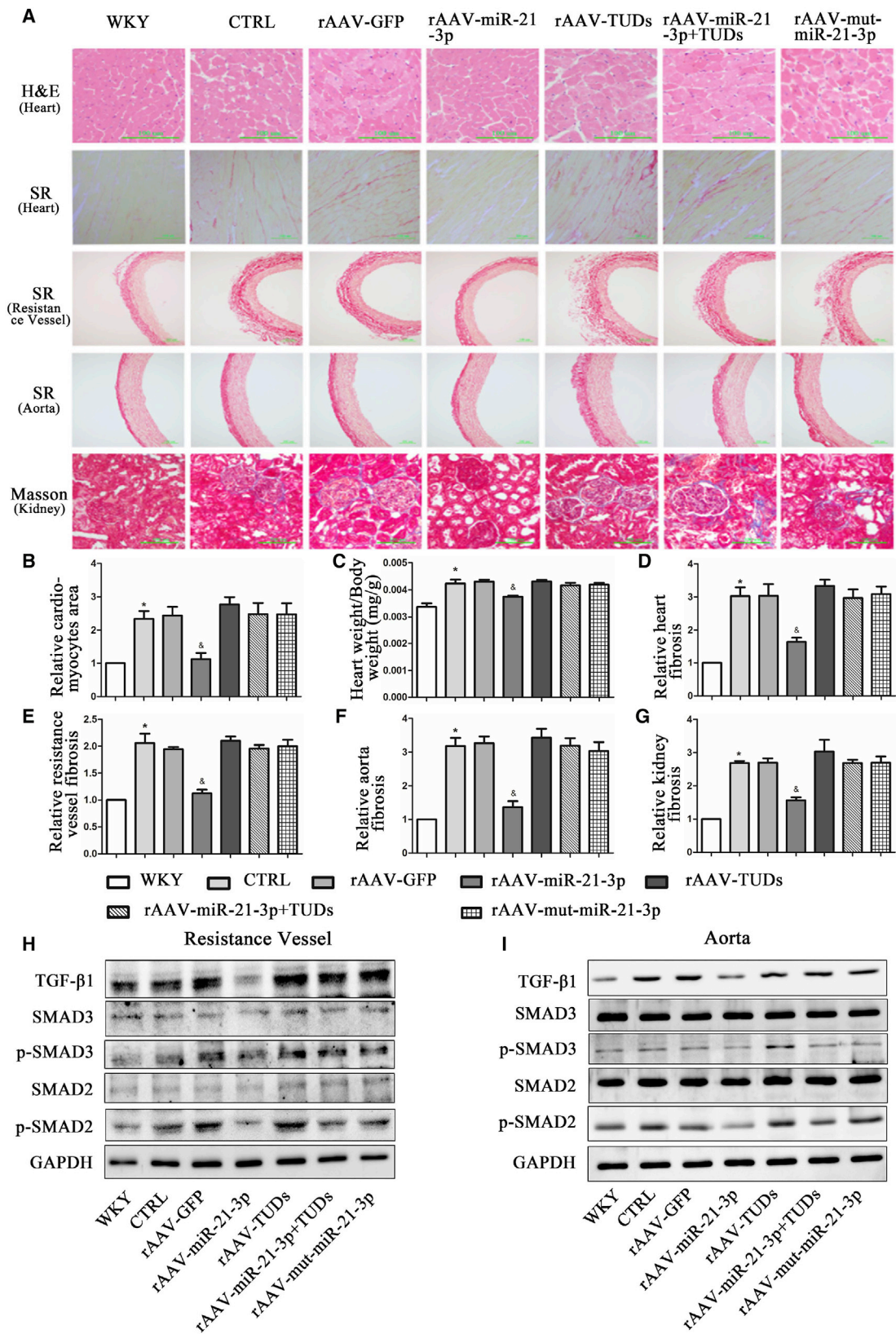
results suggest that rAAV-miR-21-3p treatment has a marked and long-term hypotensive effect in SHRs. Alternatively, the blood pressures of experimental rats were also measured by a catheter tip manometer advanced into the right carotid artery. Results showed that the blood pressures of the carotid artery were significantly reduced in rAAV-miR-21-3p-treated SHRs compared with other SHRs (Figure 2C). These data further suggest the finding that rAAV-miR-21-3p treatment significantly lowers blood pressure in SHRs.

Next, contractile responses to norepinephrine (NE) were analyzed to test the functional behavior of arteries. Cumulative addition of NE elicited a concentration-dependent contraction in the resistance vessel (mesenteric artery) and aorta from WKYs and SHRs with different treatments, respectively. A strong contractility was observed in resistance vessels from WKY rats, whereas vascular rings derived from SHRs exhibited a weaker response to NE. However, miR-21-3p markedly increased the vasoconstriction of arteries from SHRs treated with the highest concentration of NE (Figures 2D and 2E). Endothelium-dependent and -independent relaxation in the NE pre-contracted resistance vessel and aorta of experimental rats was

also performed. The relaxant effect of acetylcholine (Ach) at the maximal concentration tested was significantly increased in the resistance vessel (Figure 2F) and aorta (Figure 2G) from SHRs treated with rAAV-miR-21-3p when compared with arteries from other groups. In addition, rAAV-miR-21-3p significantly increased the endothelium-independent vasodilation to sodium nitroprusside (SNP) both in the resistance vessel (Figure 2H) and aorta (Figure 2I) from SHRs, whereas the vessels from SHRs of other groups displayed weaker capacities of the vasodilator.

Tissue Distribution of rAAV-Medicated miR-21-3p Expression in SHRs

We examined the expression profile of miR-21-3p in WKYs and SHRs, and results showed that rAAV-miR-21-3p significantly elevated miR-21-3p levels in various tissues of SHRs, including resistance vessels, aorta, brain, heart, kidney, and liver, specifically in small resistance arteries that achieved an approximately 200-fold increase (Figures S1A–S1F). Furthermore, to accurately determine the location of rAAV-mediated miR-21-3p delivery in the arteries of SHRs, rAAV-GFP-miR-21-3p was constructed and intravenously injected into SHRs. Immunofluorescence staining confirmed that



(legend on next page)

the expression of GFP was significantly increased in vascular smooth muscle cells (VSMCs) of vascular medial membrane (Figures S1G and S1H), whereas the level of miR-21-3p was also elevated there (Figures S1I and S1J). These results implied that the reduction of blood pressure induced by rAAV-miR-21-3p could be the result of increased miR-21-3p expression in VSMCs of arteries in SHR.

miR-21-3p Protects Target Organs from Damage Induced by Hypertension

Myocardial hypertrophy and fibrosis are important parts of heart injury of long-term hypertension and independent predictors for cardiovascular events in clinical practice. In the present study, our results from echocardiography showed that rAAV-miR-21-3p treatment significantly ameliorated cardiac dysfunction and reduced interventricular septum thickness in SHR (Table S3). H&E staining of myocardial tissue showed that miR-21-3p significantly reduced the sizes of the cardiac myocytes in SHR (Figures 3A and 3B). In addition, the ratio of heart weight/body weight (HW/BW) was also decreased in miR-21-3p-treated SHR compared with rAAV-GFP- or saline-treated SHR (Figure 3C). Furthermore, Sirius Red staining showed that miR-21-3p treatment significantly decreased the red-stained area of cardiac tissues compared to rAAV-GFP-treated rats (Figures 3A and 3D). However, rAAV-miR-21-3p TuDs and rAAV-mut-miR-21-3p abolished this protective effect of rAAV-miR-21-3p in the heart. All these results suggested that administration of rAAV-miR-21-3p remarkably alleviated cardiac hypertrophy and fibrosis.

Sirius Red and Masson staining of tissue sections were also performed for assessing the levels of fibrosis in the resistance vessel, aorta, and kidney during hypertension, respectively. Compared with saline control and rAAV-GFP-treated SHR, the fibrosis level of the resistance vessel (Figures 3A and 3E) and aorta (Figures 3A and 3F) in rAAV-miR-21-3p-treated SHR was significantly decreased. However, rAAV-mut-miR-21-3p and rAAV-miR-21-3p TuDs could abrogate this anti-fibrotic effect of miR-21-3p in SHR. As expected, miR-21-3p also exhibited a remarkable anti-fibrosis capacity in the kidney of SHR (Figures 3A and 3G).

To further determine the effect of miR-21-3p in the amelioration of tissue fibrosis in SHR, western blots were performed to examine the expressions of transforming growth factor β 1 (TGF- β 1), SMAD2, SMAD3, TIMP1, MMP9, and COL1 in different organs, respectively. The results showed that the protein levels of TGF- β 1, phospho-SMAD2, phospho-SMAD3, TIMP1, and COL1 were significantly increased in the resistance vessel (Figures 3H and S2C), aorta (Figures 3I and S2D), heart (Figures S2A and S2E), and kidney (Figures S2B and S2F) in SHR when compared with WKY, whereas the

level of MMP9 was markedly reduced. However, overexpression of miR-21-3p remarkably attenuated organ fibrosis in hypertension, as assessed by an increased level of MMP9 and reduced expressions of TGF- β 1, phospho-SMAD2, phospho-SMAD3, TIMP1, and COL1 in the above tissues of SHR. These observations suggested that rAAV-miR-21-3p significantly attenuated target organ fibrosis in SHR.

ADRA2B Is a Physiological Target of miR-21-3p

Via bioinformatics analysis, α 2B-adrenergic receptor (*ADRA2B*), which has been shown to play an important role in hypertension,^{38,39} was found as a putative target of miR-21-3p in both humans and rats. As previously described, rAAV-miR-21-3p significantly increased the miR-21-3p level in VSMCs of arteries and remarkably ameliorated the function of resistance vessel *in vivo*; therefore, VSMC was chosen as the target cell.

To validate the target, we performed miR-21-3p mimics and inhibitor *in vitro* experiments. Results showed that miR-21-3p mimics significantly reduced the expression of *ADRA2B* in VSMCs (Figure 4A). In addition, luciferase activity reporter assays showed that after co-transfection with miR-21-3p mimics, the relative luciferase activity of pMIR-*ADRA2B* 3' UTR was significantly suppressed compared with negative or random control, whereas the miR-21-3p inhibitor slightly increased luciferase activity. However, no change occurred after co-transfection with the pMIR mutant-*ADRA2B* 3' UTR vector (Figure 4B). Furthermore, we validated this result in experimental rats. It is recognized that *ADRA2B* is abundantly present in the vasculature, brain, and kidney. We therefore examined the protein levels of *ADRA2B* in resistance vessels, aorta, brain, and kidney from WKY and SHR, respectively. Western blots showed that miR-21-3p treatment significantly down-regulated the expressions of *ADRA2B* in resistance vessels (Figure 4C), aorta (Figure 4D), brain (Figure 4E), and kidney (Figure 4F) *in vivo*. Moreover, to provide more evidence, we performed a binding assay by immunoprecipitated Ago2-containing complexes. Results showed that the RNA levels of miR-21-3p and *ADRA2B*, co-immunoprecipitated with Ago2 protein, were significantly increased compared with control (Figure 4G), suggesting that miR-21-3p targets *ADRA2B* by directly binding with its 3' UTR. Collectively, these results strongly suggested that *ADRA2B* was an important physiological target of miR-21-3p.

miR-21-3p Regulates the Phenotypic Switch of VSMCs via *ADRA2B* and Ameliorates Vascular Remodeling in Hypertension

Vascular remodeling contributes to increased peripheral resistance and plays a pivotal role in the development of hypertension.⁴⁰ Recently, accumulating evidence revealed that miRNAs had abilities

Figure 3. Influence of miR-21-3p on the Protection of Target Organ Damage Induced by Hypertension in SHR

(A) Representative images of morphological staining in various tissues from WKY and SHR. (B) Quantitative analysis of the cardiomyocyte area. (C) HW/BW ratio. (D–G) Quantitative analysis of tissue fibrosis of the heart (D), resistance vessel (E), aorta (F), and kidney (G), respectively. (H and I) Protein expression of TGF- β 1, SMAD2, p-SMAD2, SMAD3, and p-SMAD3 in resistance vessels (H) and aorta (I) from WKY and SHR with different treatments. CTRL, SHR-Control (treated with normal saline); SR, Sirius Red. Data are presented as mean \pm SEM ($n \geq 3$); * $p < 0.05$ versus WKYs; [#] $p < 0.05$ versus SHR control.

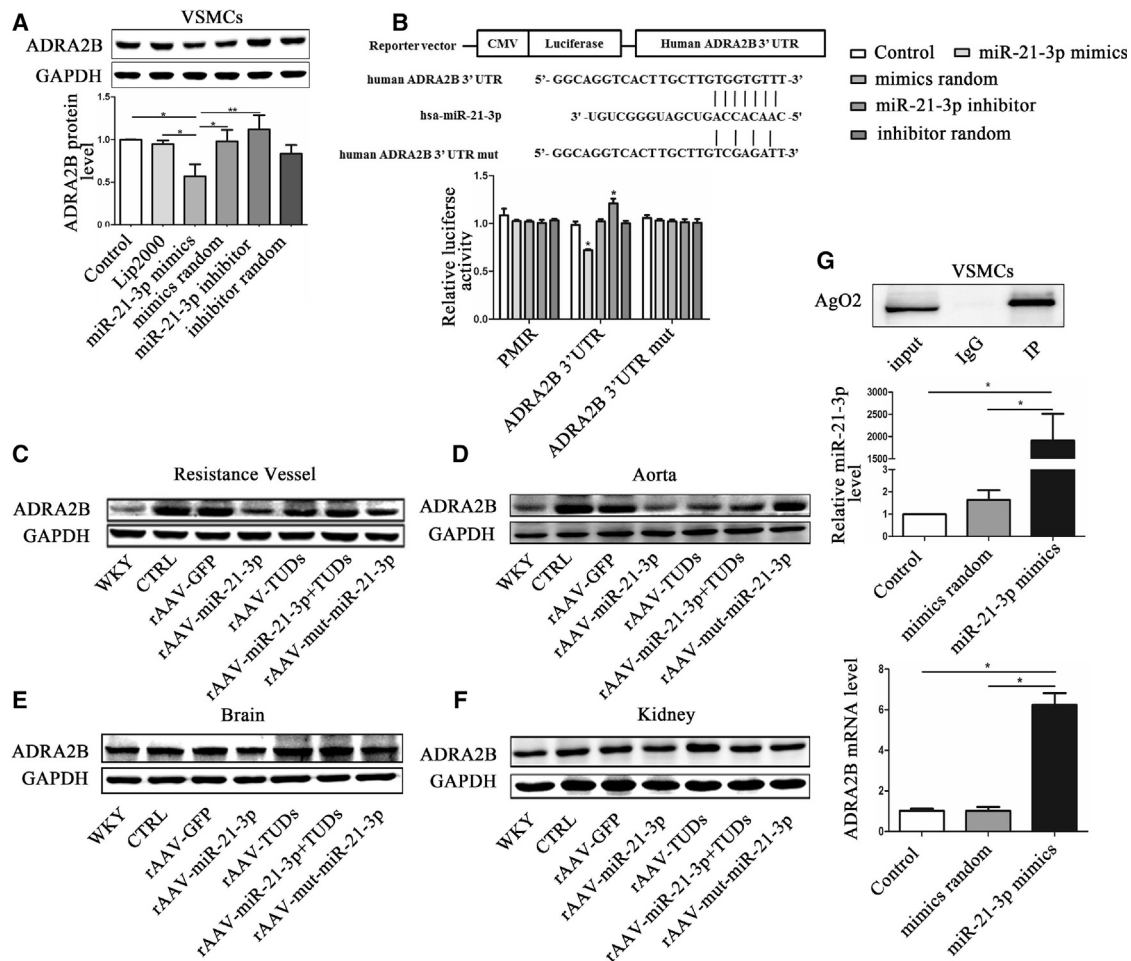
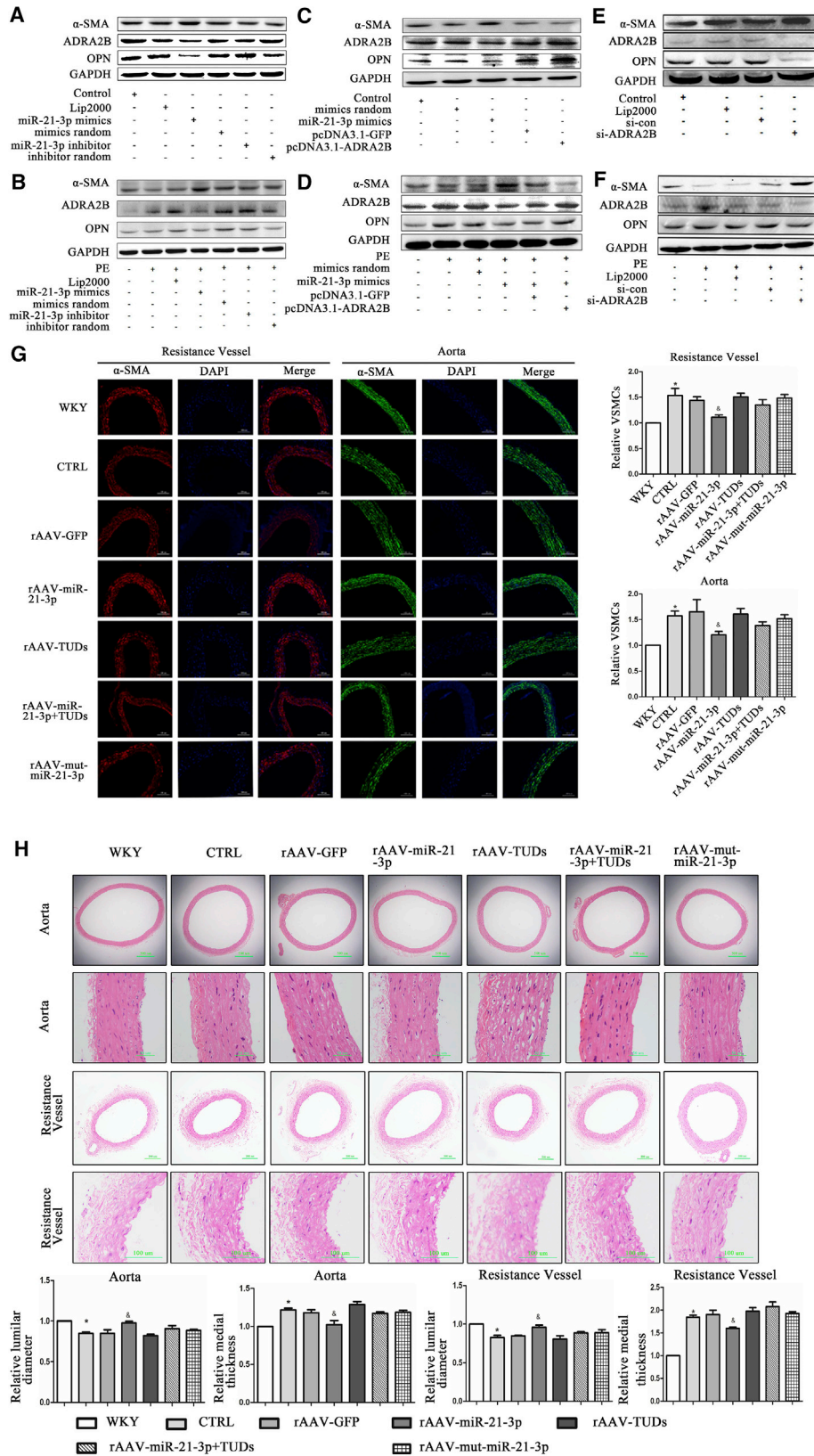


Figure 4. miR-21-3p Negatively Regulates the Expression of ADRA2B

(A) The expression of ADRA2B protein in VSMCs. (B) The luciferase activity of pMIR-ADRA2B 3' UTR plasmid in the 239T cell after co-transfection with miR-21-3p mimics. (C–F) The expression of ADRA2B protein in the resistance vessel (C), aorta (D), brain (E), and kidney (F), respectively. (G) The level of ADRA2B mRNA captured by co-immunoprecipitation after administration with miR-21-3p mimics in VSMCs. CTRL, SHR-Control (treated with normal saline); PMIR, pMIR empty plasmid. Data are presented as mean \pm SEM ($n \geq 3$); * $p < 0.05$; ** $p < 0.01$.

to control the proliferation, differentiation, and phenotypic switching of VSMCs.^{30,41,42} In the present study, to confirm whether miR-21-3p was able to regulate the phenotype switch of VSMCs in hypertension, a number of markers specific for contractile VSMC (α -SMA) and synthetic VSMC (OPN) were examined. Phenylephrine (PE) was used to mimic the environment of high pressure *in vitro*. Results showed that miR-21-3p mimics significantly stimulated the contractile type of VSMCs, as assessed by an increased level of α -SMA and reduced expression of OPN in VSMCs (Figure 5A). Furthermore, VSMCs were exposed to a high-pressure environment induced by PE. Interestingly, we found that PE markedly increased ADRA2B level in VSMCs and induced a switch from contractile VSMC to synthetic VSMC. However, miR-21-3p significantly attenuated this effect induced by PE in VSMCs (Figure 5B). Moreover, we investigated whether the effect of miR-21-3p in the switch of VSMC phenotype was mediated by ADRA2B. Western blots showed that overexpression

of ADRA2B increased OPN in VSMCs, whereas the level of α -SMA was reduced (Figures 5C and 5D). However, silencing of ADRA2B by small interfering RNAs (siRNAs) significantly reduced OPN level and elevated the expression of α -SMA (Figures 5E and 5F). These results suggest that miR-21-3p may regulate phenotype switch of VSMCs via ADRA2B. It has been reported that the phenotype switch of VSMCs from contraction type to synthetic type may induce VSMC proliferation,⁴¹ and accelerated proliferation of VSMCs is closely linked with hypertension.⁴³ Furthermore, to test the effects of miR-21-3p on proliferation of VSMCs *in vivo*, we analyzed the number of VSMCs in the resistance vessel and aorta from WKYs and SHRs by immunofluorescence staining. The relative quantitative morphometric analysis revealed that the VSMC numbers of the resistance vessel and aorta in SHRs were much higher than in WKYs (Figure 5G). However, miR-21-3p significantly suppressed the excessive proliferation of VSMCs in the arteries of SHRs (Figure 5G).



(legend on next page)

Moreover, medial thickness and luminal diameter of the resistance vessel and aorta have been used for estimating arterial remodeling. Both in the resistance artery and aorta, we detected an obvious vascular remodeling in SHR compared with WKYs, as shown by increased medial thickness and reduced luminal diameter, whereas miR-21-3p significantly decreased medial thickness and increased luminal diameter in the arteries of SHR (Figure 5H). The above mentioned results suggested that miR-21-3p repressed phenotypic switching of VSMCs (from contractile type to synthetic type), inhibited VSMCs proliferation, and consequently ameliorated vascular remodeling in hypertension.

AGTR1 and RHOB Are Potential Targets of miR-21-3p in Humans

Interestingly, besides *ADRA2B*, the genes of angiotensin II receptor type 1 (*AGTR1*) and Ras homolog family member B (*RHOB*), associated with arterial hypertension and pulmonary hypertension, were also predicted as potential targets of miR-21-3p only in humans. Western blot showed that miR-21-3p mimics significantly decreased the protein levels of *AGTR1* and *RHOB* (Figure S3A) in human umbilical vein endothelial cells (HUVECs). Transfection of pMIR-*AGTR1* 3' UTR or pMIR-*RHOB* 3' UTR with miR-21-3p mimics into 293T cells resulted in a significant reduction of luciferase activity compared with control and the random group (Figure S3B and S3C). Ago2 co-immunoprecipitation further supported that *AGTR1* and *RHOB* were potential targets of hsa-miR-21-3p (Figure S3D).

Expression of miR-21-3p Is Regulated by the Transcription Factor

Ever increasing studies have demonstrated that the expressions of miRNAs are regulated by transcription factors.^{44,45} We selected several transcription factors associated with cardiovascular diseases, such as nuclear factor κ B (NF- κ B), SRF, Sp1, AP-1, GATA-4, and Nrf2, and looked at their expressions in resistance vessels. Our results showed that the levels of expression of NF- κ B, Sp1, and Nrf2 were significantly increased in SHR than in WKYs, whereas the levels of SRF, AP-1, and GATA-4 were obviously reduced (Figure 6A). To further investigate whether the expression of miR-21-3p was regulated by the transcription factors mentioned above, a bioinformatics search (Alibaba 2.1) was performed to confirm the transcription factor binding sites in the upstream sequence (~2,000 bp) of the miR-21-3p promoter. Interestingly, we found that *NF- κ B*, *SRF*, *Sp1*, *AP-1*, and *Nrf2* might have binding sites in the miR-21-3p promoter but not *GATA4*, so we selected *NF- κ B p65* and *SRF*, which were predicted with a higher score of binding in the miR-21-3p promoter by bioinformatics analyses as the representatives.

NF- κ B p65

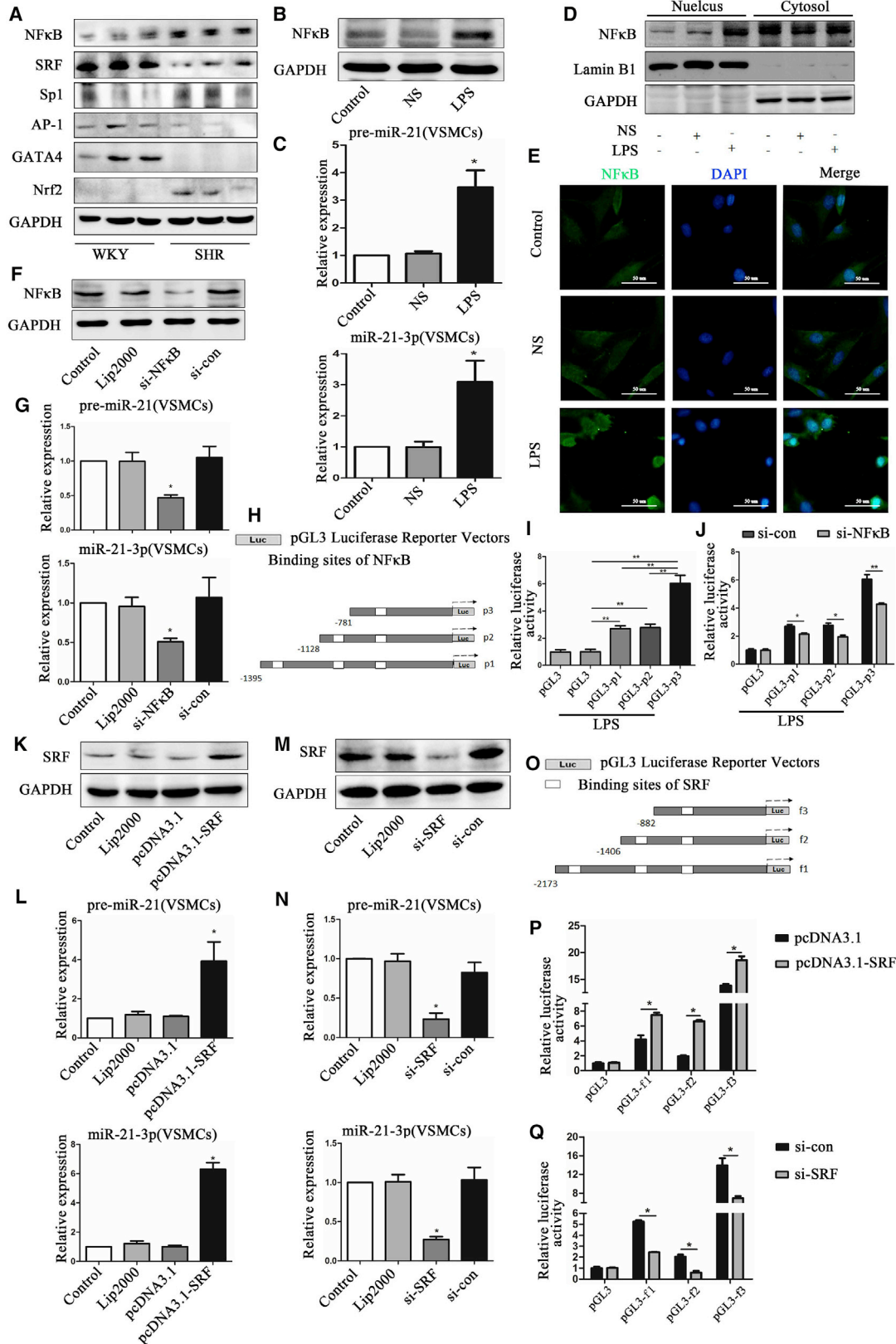
Western blot and qRT-PCR analysis showed that lipopolysaccharide (LPS) significantly increased the cellular levels of precursor-miR-21 and mature miR-21-3p by elevating p65 protein expression and activating *NF- κ B* signaling via translocation of p65 to the nucleus in both VSMCs (Figures 6B–6E) and HUVEC (Figures S4A–S4C). However, in contrast, *NF- κ B* siRNA dramatically reduced the cellular levels of precursor-miR-21 and mature miR-21-3p by suppressing the protein expression and nuclear translocation of p65 in VSMCs (Figures 6F and 6G) and HUVEC (Figure S4D). In addition, to exactly localize the binding sites of *NF- κ B* in miR-21-3p upstream, three promoter segments of the miR-21-3p transcript with different lengths (–1,395 to –18, –1,128 to –18, and –781 to –18) confirmed by DNA sequencing were cloned into the pGL3 luciferase reporter vector, respectively (Figure 6H). Dual-luciferase assays showed that the relative luciferase activity of pGL3-p1, pGL3-p2, and pGL3-p3 was significantly increased after treatment of LPS compared with pGL3 control, and the highest luciferase activity was presented in pGL3-p3 (Figure 6I). Furthermore, transfection of *NF- κ B* siRNA significantly reduced the elevated luciferase activity of pGL3-p1, pGL3-p2, and pGL3-p3 induced by LPS (Figure 6J). These data suggested that the major binding site of *NF- κ B* was located in the region of –469 to –460 bp in the miR-21-3p gene upstream.

SRF

As shown in Figures 6K and 6L, overexpression of SRF by the pcDNA 3.1-SRF plasmid significantly increased the expressions of precursor-miR-21 and mature miR-21-3p in VSMCs. However, reduction of *SRF* gene expression by *SRF* siRNA resulted in decreased levels of precursor-miR-21 and mature miR-21-3p in VSMCs (Figures 6M and 6N). Bioinformatics analyses revealed that there are three different binding sites of *SRF* in miR-21-3p upstream (~2,000 bp) as well as *NF- κ B*. Moreover, to validate the binding sites of *SRF* in the miR-21-3p promoter, three promoter segments of miR-21-3p transcript with different lengths (–2,173 to +94, –1,406 to +94, and –882 to +94) were inserted into the pGL3 luciferase reporter vector and denoted by pGL3-f1, pGL3-f2, and pGL3-f3, respectively (Figure 6O). Our results revealed that the relative luciferase activity of pGL3-f1, pGL3-f2, and pGL3-f3 were obviously elevated after co-transfection with pcDNA 3.1-SRF plasmid, and the highest luciferase activity was presented in pGL3-f3 (Figure 6P). However, treatment of *SRF* siRNA significantly reduced the elevated luciferase activity of pGL3-f1, pGL3-f2, and pGL3-f3 compared with normal control (Figure 6Q). These data suggested that the major binding site of *SRF* was

Figure 5. miR-21-3p Regulates the Phenotypic Switch of VSMCs and Ameliorates Vascular Remodeling in Hypertension

(A and B) The expressions of α -SMA, ADRA2B, and OPN in VSMCs stimulated by miR-21-3p mimics treated with (B) or without (A) PE. (C and D) The expressions of α -SMA, ADRA2B, and OPN in VSMCs after administration with miR-21-3p mimics or pcDNA 3.1-ADRA2B plasmid treated with (D) or without (C) PE. (E and F) The expressions of α -SMA, ADRA2B, and OPN in VSMCs after co-transfection with ADRA2B-siRNA treated with (F) or without PE (E). (G) Immunofluorescence staining of the resistance vessel (α -SMA, red; nuclei, blue) and aorta (α -SMA, green; nuclei, blue) from WKYs and SHR with different treatments. (H) H&E staining of the aorta and resistance vessel from WKYs and SHR with different treatments; medial thickness and luminal diameter were quantified using morphometry. CTRL, SHR-Control (treated with normal saline); lip2000, lipofectamine 2000; PE, phenylephrine; siRNA-con, siRNA negative control. Data are presented as mean \pm SEM (n \geq 3); *p < 0.05 versus WKYs; [#]p < 0.05 versus SHR control.



(legend on next page)

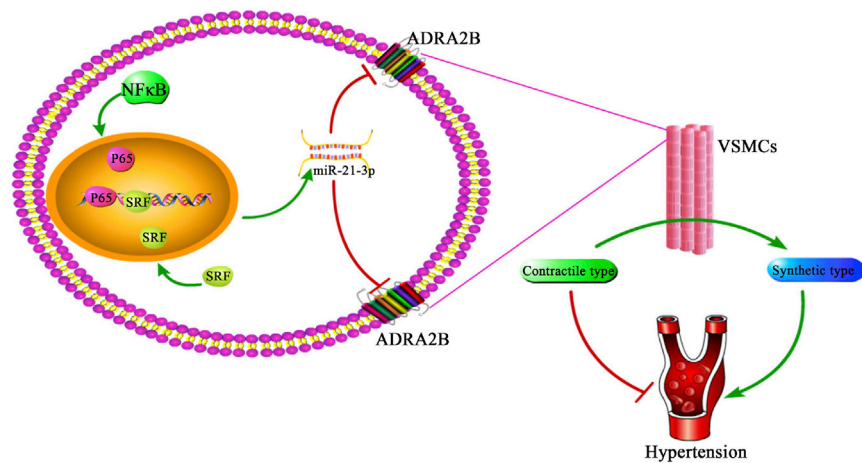


Figure 7. The Role of miR-21-3p in Hypertension

Elevated miR-21-3p by rAAV-mediated delivery significantly decreases the blood pressure of SHR by directly suppressing the expression of *ADRA2B* and protects target organ damages associated with hypertension. In addition, activation of *NF-κB* and *SRF* signaling remarkably increase the expression of miR-21-3p by directly binding with the promoter of the miR-21-3p gene.

located in the region of -860 to -843 bp in the miR-21-3p gene upstream.

DISCUSSION

In the present study, the abnormal expression of miR-21-3p has been identified in hypertension patients, and its level negatively correlated with blood pressure level *in vivo*, suggesting miR-21-3p is involved in hypertension. rAAV-mediated miR-21-3p delivery significantly ameliorated hypertension via attenuating the expression of *ADRA2B* in VSMCs of arteries and alleviated target organ damages in a hypertensive animal model. Sponge absorption of miR-21-3p by miR-21-3p TuDs abolished this hypotensive effect. In addition, we revealed that transcription factor *NF-κB* and *SRF* directly regulated the expression of miR-21-3p via binding with the promoter of the miR-21-3p gene (Figure 7).

In recent years, increasing studies clarified that miRNAs are perceived as novel therapeutic strategies in the cardiovascular diseases based on their crucial roles in various cardiovascular systems.^{46–48} miRNA mimics, synthetic double-stranded miRNA analogs, are used to regulate gene expression by simulating the miRNA-mediated gene silencing.⁴⁹ However, miRNA mimics have not yet demonstrated efficacy *in vivo*, and their development has lagged far behind the anti-miRNA chemistries.⁴⁶ Thus, some new and efficient approaches

are needed for enhancing expressions of miRNAs *in vivo*. AAV vector, with low toxicity and antigenicity, is a promising vehicle for gene therapy. A previous study showed that overexpression of miRNA “tough decoys” (TuDs) mediated by rAAV can efficiently inhibit the function of miRNAs in mice long-term.⁵⁰ In the present study, therefore, we constructed different rAAV vectors to investigate the roles and functions of differentially expressed miR-21-3p in hypertension. Importantly, we found that rAAV-miR-21-3p significantly increased the expressions of miR-21-3p in various tissues of SHR, specifically in VSMCs of arteries. Moreover, rAAV-miR-21-3p treatment significantly reduced elevated blood pressure and ameliorated cardiac hypertrophy, vascular remodeling, and organ fibrosis in SHR. However, these protective effects of miR-21-3p were abolished by injection of rAAV-miR-21-3p TuDs.

ADRA2B is an important member of the family of G-protein-coupled receptors that mediate the biological functions of endogenous catecholamines, epinephrine, and norepinephrine.⁵¹ Previous studies demonstrated that *ADRA2B* was highly expressed in the central nervous and peripheral micro-vascular systems, and was confirmed to play a crucial role in regulating blood pressure and controlling vascular tone.^{38,52,53} Long-term inhibition of the central *ADRA2B* gene by rAAV-mediated antisense significantly declined the blood pressure of hypertensive rats.⁵⁴ In this study, *ADRA2B* was identified as an important target of miR-21-3p. Further, we confirmed that elevated miR-21-3p significantly reduced the level of *ADRA2B* in the brain *in vivo*, and that may be one of the potential mechanisms of miR-21-3p in lowering blood pressure. However, in the present

Figure 6. Transcription Factor *NF-κB* and *SRF* Regulate the Expression of miR-21-3p in VSMCs

(A) The expression of transcription factors *NF-κB*, *SRF*, Sp1, AP-1, GATA-4, and Nrf2 in SHR and WKYs. (B) The expression of *NF-κB* p65 protein in VSMCs after stimulation by LPS. (C) The expression of precursor-miR-21 and mature miR-21-3p in VSMCs after stimulation by LPS. (D) The nuclear translocation of p65 in VSMCs after stimulation by LPS. (E) Immunofluorescence staining of VSMCs treated with or without LPS (*NF-κB*, green; nuclei, blue). (F) The expression of *NF-κB* p65 protein in VSMCs after co-transfection with *NF-κB* siRNA. (G) The expression of precursor-miR-21 and mature miR-21-3p in VSMCs after co-transfection with *NF-κB* siRNA. (H) Construction of three promoter segments of the miR-21-3p transcript with different binding sites of *NF-κB*. (I) The luciferase activity of pGL3-p1, pGL3-p2, and pGL3-p3 reporter plasmids stimulated by LPS. (J) The luciferase activity of pGL3-p1, pGL3-p2, and pGL3-p3 reporter plasmids after co-transfection with *NF-κB* siRNA. (K) The expression of *SRF* protein in VSMCs after co-transfection with pcDNA3.1-*SRF*. (L) The expression of precursor-miR-21 and mature miR-21-3p in VSMCs after co-transfection with pcDNA3.1-*SRF*. (M) The expression of *SRF* protein in VSMCs after co-transfection with *SRF* siRNA. (N) The expression of precursor-miR-21 and mature miR-21-3p after co-transfection with *SRF* siRNA. (O) Construction of three promoter segments of the miR-21-3p transcript with different binding sites of *SRF*. (P) The luciferase activity of pGL3-f1, pGL3-f2, and pGL3-f3 reporter plasmids co-transfected with pcDNA3.1-*SRF*. (Q) The luciferase activity of pGL3-f1, pGL3-f2, and pGL3-f3 reporter plasmids after co-transfection with *SRF* siRNA. Lip2000, lipofectamine 2000; NS, saline; si-con, siRNA-negative control. Data are presented as mean \pm SEM ($n \geq 3$); * $p < 0.05$; ** $p < 0.01$.

study, the highest expression of miR-21-3p mediated by rAAV was located in the VSMCs of arteries; thus, VSMCs are the target cells in our study. We focused on identifying the roles of miR-21-3p in vascular function and remodeling by directly targeting *ADRA2B* in the arterial. It is well established that the contractile phenotype of VSMCs, which plays an important role in controlling the diameter of blood vessels, regulating organ blood flow, and keeping a stable blood pressure is essential in the development and maintenance of a normal and mature vasculature.⁵⁵ The switch of VSMC from contractile type to synthetic type may contribute to vascular remodeling in hypertension.⁴¹ Importantly, in this study, we confirmed that miR-21-3p has the ability to control the phenotype switch of VSMCs by directly regulating the expression of *ADRA2B*, which may be the major mechanism of the miR-21-3p-mediated anti-hypertensive effect in arteries during hypertension.

Meanwhile, in the present study, we also demonstrated that *AGTRI* and *RHOB* were the targets of miR-21-3p only in humans. These results may provide more evidence to support the conclusion that miR-21-3p plays an important role in regulating blood pressure.

In the current study, we discovered that overexpression of miR-21-3p mediated by rAAV vectors significantly reduced blood pressure in SHR. However, at present, most applications of rAAV-vector-mediated gene delivery still stayed at pre-clinical. Some other approaches, which could be easily achieved, are needed to increase the level of miR-21-3p *in vivo*. Previous studies clarified that a statin has the ability to regulate the expressions of miRNAs.^{56,57} Increasing studies determined that the levels of miRNAs are regulated by a transcription factor.^{11,58} In the present study, we explored the transcriptional regulation of miR-21-3p upstream and hope to find that some drugs or transcription factors have the ability to activate endogenous miR-21-3p expression *in vivo*. Combining western blotting and bioinformatics analyses, we found that the expressions of six transcription factors (NF- κ B, SRF, Sp1, AP-1, GATA-4, and Nrf2) were changed in hypertension, and most of them have been predicted to bind with the miR-21-3p promoter region. These results suggested that the above transcription factors might be involved in the regulation of miR-21-3p expression. It was reported that NF- κ B was associated with hypertension,⁵⁹ and previous studies demonstrated that SRF was involved in phenotypic switch of VSMCs.^{60,61} Furthermore, both of them were predicted with a higher score of binding in the miR-21-3p promoter by a bioinformatics analysis. So NF- κ B p65 and SRF were selected as the representative transcription factors of miR-21-3p in the subsequent study. Our results demonstrated the important roles of NF- κ B and SRF in the regulation of miR-21-3p expression. Furthermore, using promoter deletion analysis, we finally confirmed that the major binding site of NF- κ B and SRF was located in the region of -469 to -460 bp and -860 to -843 bp of the miR-21-3p transcript upstream, respectively. Together, we found that the regulation of miR-21-3p expression was very complex because various transcription factors may participate. Some of them may upregulate the expression of miR-21-3p, whereas others may downregulate. All these ef-

fects ultimately lead to the downregulation of miR-21-3p expression in SHR.

In short, our data revealed, in part, the complex regulatory mechanisms of miR-21-3p expression and provided some potential theoretical basis for controlling blood pressure by regulating the level of miR-21-3p *in vivo*.

In summary, we showed that the level of circulating miR-21-3p was reduced both in hypertension patients and hypertensive rats. rAAV-mediated miR-21-3p overexpression significantly attenuated blood pressure in hypertension and weakened target organ damages associated with hypertension. Therefore, our findings provide a possibility of gene therapy for hypertension by rAAV-miR-21-3p.

MATERIALS AND METHODS

Population

All the participants in this study were admitted to the Cardiovascular Division in Tongji Hospital between September 2012 and May 2013, and 5-mL blood samples were collected via venous puncture after written informed consent was obtained from them. After isolation by centrifugation, the plasma was transferred to RNase-free tubes and stored at -80°C until being further processed. This study was conducted in accordance with the Declaration of Helsinki and approved by the Ethics Committee of Tongji Hospital.

Construction and Preparation of rAAV

The rAAV-D(+) vector (double-stranded rAAV vector plasma), adenovirus helper plasmid phelper, and packaging plasmid pXX9 were provided kindly by Dr. Xiao Xiao and have been described previously.⁶² Packages and purification of rAAVs were performed as described previously.^{62,63} The eluted rAAV was aliquoted and stored at -80°C for animal administration.

Experimental Animals

SHRs and WKYs were purchased from the Vital River Laboratory Animal Technology Company (supported by Charles River Laboratories) in Beijing. During the whole study period, the animals were housed at room temperature with 12-hr light/dark cycles and allowed free access to normal rat chow and water *ad libitum*. The animal experimental protocols complied with standards stated from NIH Guidelines for the Care and Use of Laboratory Animals and the Chinese Academy of Sciences and were approved by the Tongji Hospital Ethics Committee.

Measurement of Blood Pressure

The systolic blood pressure of rats was measured by a noninvasive sphygmomanometer (BP-2010A, Softron Biotechnology, Beijing, China) via cuffing the tails. The systolic blood pressures of WKYs and SHRs were measured every 2 weeks at the first 2 months after administration with rAAVs and were monitored every 2 or 3 weeks after 16 weeks of age while the level of blood pressure became stable. For each measurement, the systolic blood pressure was represented as the mean of at least 5 stable recordings.

The carotid arterial pressures of rats were also detected at the end of the experiment. A catheter tip manometer (AD Instruments, Bella Vista, NSW, Australia) was advanced into the right carotid artery for monitoring the blood pressure of the carotid artery.

Statistical Analysis

Relative expression levels of miRNAs were calculated by the $2^{-\Delta\Delta ct}$ method. Data are expressed as mean \pm SEM unless otherwise indicated. The data of blood pressure and function of the vascular system in all experimental rats over the time course were statistically analyzed by repeated-measured ANOVA. Concentration-dependent contractile response to NE was recorded as the percentage of the maximal contraction obtained with high K^+ relaxation responses to cumulative concentrations of Ach and SNP and calculated as percentage inhibition of NE-induced peak contraction. Student's t test (2 groups) and ANOVA (n groups) were used for analyzing normally distributed variables. Mann-Whitney U test (2 groups) and Kruskal-Wallis test (n groups) were performed as appropriate for assessing non-normally distributed variables. Categorical variables were analyzed by χ^2 test. Correlation analysis was determined by Spearman correlation analysis. All statistical calculations were accomplished by SPSS 17.0 software, and $p < 0.05$ (two-sided) was considered a statistically significant difference.

SUPPLEMENTAL INFORMATION

Supplemental Information includes Supplemental Materials and Methods, four figures, and four tables and can be found with this article online at <https://doi.org/10.1016/j.omtn.2017.11.007>.

AUTHOR CONTRIBUTIONS

All authors have approved this manuscript and its contents and they are aware of the responsibilities connected with authorship. F.W. and Q.F. designed and performed the study and analyzed the data; C.C., L.Z., H.L., Y.Z., Y.W., C.X.Z., and X.X. participated in performing the study; D.W.W. designed and organized the study.

CONFLICTS OF INTEREST

The authors declare no competing financial interests.

ACKNOWLEDGMENTS

We thank Dr. Xiao Xiao for kind provision of recombinant adeno-associated virus. This work was supported by the National Natural Science Foundation of China (grants 91439203, 81630010, 81500327, and 81500328).

REFERENCES

- Te Riet, L., van Esch, J.H., Roks, A.J., van den Meiracker, A.H., and Danser, A.H. (2015). Hypertension: renin-angiotensin-aldosterone system alterations. *Circ. Res.* *116*, 960–975.
- Parati, G., and Esler, M. (2012). The human sympathetic nervous system: its relevance in hypertension and heart failure. *Eur. Heart J.* *33*, 1058–1066.
- DiBona, G.F. (2013). Sympathetic nervous system and hypertension. *Hypertension* *61*, 556–560.

- Paravicini, T.M., and Touyz, R.M. (2006). Redox signaling in hypertension. *Cardiovasc. Res.* *71*, 247–258.
- Intengan, H.D., and Schiffrin, E.L. (2001). Vascular remodeling in hypertension: roles of apoptosis, inflammation, and fibrosis. *Hypertension* *38*, 581–587.
- Feihl, F., Liaudet, L., Levy, B.I., and Waeber, B. (2008). Hypertension and microvascular remodelling. *Cardiovasc. Res.* *78*, 274–285.
- Egan, B.M., Zhao, Y., Axon, R.N., Brzezinski, W.A., and Ferdinand, K.C. (2011). Uncontrolled and apparent treatment resistant hypertension in the United States, 1988 to 2008. *Circulation* *124*, 1046–1058.
- Persell, S.D. (2011). Prevalence of resistant hypertension in the United States, 2003–2008. *Hypertension* *57*, 1076–1080.
- Bartel, D.P. (2004). MicroRNAs: genomics, biogenesis, mechanism, and function. *Cell* *116*, 281–297.
- Winter, J., Jung, S., Keller, S., Gregory, R.I., and Diederichs, S. (2009). Many roads to maturity: microRNA biogenesis pathways and their regulation. *Nat. Cell Biol.* *11*, 228–234.
- Hermeking, H. (2007). p53 enters the microRNA world. *Cancer Cell* *12*, 414–418.
- Carthew, R.W., and Sontheimer, E.J. (2009). Origins and mechanisms of miRNAs and siRNAs. *Cell* *136*, 642–655.
- Takashima, Y., Terada, M., Udono, M., Miura, S., Yamamoto, J., and Suzuki, A. (2016). Suppression of lethal-7b and miR-125a/b maturation by Lin28b enables maintenance of stem cell properties in hepatoblasts. *Hepatology* *64*, 245–260.
- Nakagawa, R., Leyland, R., Meyer-Hermann, M., Lu, D., Turner, M., Arbore, G., Phan, T.G., Brink, R., and Vigorito, E. (2016). MicroRNA-155 controls affinity-based selection by protecting c-MYC+ B cells from apoptosis. *J. Clin. Invest.* *126*, 377–388.
- Murai, K., Sun, G., Ye, P., Tian, E., Yang, S., Cui, Q., Sun, G., Trinh, D., Sun, O., Hong, T., et al. (2016). The TLX-miR-219 cascade regulates neural stem cell proliferation in neurodevelopment and schizophrenia iPSC model. *Nat. Commun.* *7*, 10965.
- Small, E.M., Frost, R.J., and Olson, E.N. (2010). MicroRNAs add a new dimension to cardiovascular disease. *Circulation* *121*, 1022–1032.
- Thum, T., and Condorelli, G. (2015). Long noncoding RNAs and microRNAs in cardiovascular pathophysiology. *Circ. Res.* *116*, 751–762.
- Hodgkinson, C.P., Kang, M.H., Dal-Pra, S., Mirosou, M., and Dzau, V.J. (2015). MicroRNAs and Cardiac Regeneration. *Circ. Res.* *116*, 1700–1711.
- Ganesan, J., Ramanujam, D., Sassi, Y., Ahles, A., Jentsch, C., Werfel, S., Leierseder, S., Loyer, X., Giacca, M., Zentilin, L., et al. (2013). MiR-378 controls cardiac hypertrophy by combined repression of mitogen-activated protein kinase pathway factors. *Circulation* *127*, 2097–2106.
- van Rooij, E., Sutherland, L.B., Thatcher, J.E., DiMaio, J.M., Naseem, R.H., Marshall, W.S., Hill, J.A., and Olson, E.N. (2008). Dysregulation of microRNAs after myocardial infarction reveals a role of miR-29 in cardiac fibrosis. *Proc. Natl. Acad. Sci. USA* *105*, 13027–13032.
- Nagpal, V., Rai, R., Place, A.T., Murphy, S.B., Verma, S.K., Ghosh, A.K., and Vaughan, D.E. (2016). MiR-125b is critical for fibroblast-to-myofibroblast transition and cardiac fibrosis. *Circulation* *133*, 291–301.
- Castaldi, A., Zaglia, T., Di Mauro, V., Carullo, P., Viggiani, G., Borile, G., Di Stefano, B., Schiattarella, G.G., Gualazzi, M.G., Elia, L., et al. (2014). MicroRNA-133 modulates the β 1-adrenergic receptor transduction cascade. *Circ. Res.* *115*, 273–283.
- Flemming, A. (2014). Heart failure: targeting miRNA pathology in heart disease. *Nat. Rev. Drug Discov.* *13*, 336.
- Wahlquist, C., Jeong, D., Rojas-Muñoz, A., Kho, C., Lee, A., Mitsuyama, S., van Mil, A., Park, W.J., Sluijter, J.P., Doevendans, P.A., et al. (2014). Inhibition of miR-25 improves cardiac contractility in the failing heart. *Nature* *508*, 531–535.
- Fiedler, J., Jazbutyte, V., Kirchmaier, B.C., Gupta, S.K., Lorenzen, J., Hartmann, D., Galuppo, P., Kneitz, S., Pena, J.T., Sohn-Lee, C., et al. (2011). MicroRNA-24 regulates vascularity after myocardial infarction. *Circulation* *124*, 720–730.
- Wang, K., Zhou, L.Y., Wang, J.X., Wang, Y., Sun, T., Zhao, B., Yang, Y.J., An, T., Long, B., Li, N., et al. (2015). E2F1-dependent miR-421 regulates mitochondrial fragmentation and myocardial infarction by targeting Pink1. *Nat. Commun.* *6*, 7619.
- Fiedler, J., and Thum, T. (2016). New insights into miR-17-92 cluster regulation and angiogenesis. *Circ. Res.* *118*, 9–11.

28. Feinberg, M.W., and Moore, K.J. (2016). MicroRNA regulation of atherosclerosis. *Circ. Res.* *118*, 703–720.
29. Parikh, V.N., Jin, R.C., Rabello, S., Gulbahce, N., White, K., Hale, A., Cottrill, K.A., Shaik, R.S., Waxman, A.B., Zhang, Y.Y., et al. (2012). MicroRNA-21 integrates pathogenic signaling to control pulmonary hypertension: results of a network bioinformatics approach. *Circulation* *125*, 1520–1532.
30. Shi, L., Liao, J., Liu, B., Zeng, F., and Zhang, L. (2015). Mechanisms and therapeutic potential of microRNAs in hypertension. *Drug Discov. Today* *20*, 1188–1204.
31. Carr, G., Barrese, V., Stott, J.B., Povstyan, O.V., Jepps, T.A., Figueiredo, H.B., Zheng, D., Jamshidi, Y., and Greenwood, I.A. (2016). MicroRNA-153 targeting of KCNQ4 contributes to vascular dysfunction in hypertension. *Cardiovasc. Res.*, Published online July 7, 2016. <https://doi.org/10.1093/cvr/cvw177>.
32. Zhu, Q., Hu, J., Wang, L., Wang, W., Wang, Z., Li, P.L., Boini, K.M., and Li, N. (2017). Inhibition of microRNA-429 in the renal medulla increased salt sensitivity of blood pressure in Sprague Dawley rats. *J. Hypertens.* *35*, 1872–1880.
33. Yan, M., Chen, C., Gong, W., Yin, Z., Zhou, L., Chaugai, S., and Wang, D.W. (2015). miR-21-3p regulates cardiac hypertrophic response by targeting histone deacetylase-8. *Cardiovasc. Res.* *105*, 340–352.
34. Ro, S., Park, C., Young, D., Sanders, K.M., and Yan, W. (2007). Tissue-dependent paired expression of miRNAs. *Nucleic Acids Res.* *35*, 5944–5953.
35. Griffiths-Jones, S., Hui, J.H., Marco, A., and Ronshaugen, M. (2011). MicroRNA evolution by arm switching. *EMBO Rep.* *12*, 172–177.
36. Yang, J.S., Phillips, M.D., Betel, D., Mu, P., Ventura, A., Siepel, A.C., Chen, K.C., and Lai, E.C. (2011). Widespread regulatory activity of vertebrate microRNA* species. *RNA* *17*, 312–326.
37. Li, H., Zhang, X., Wang, F., Zhou, L., Yin, Z., Fan, J., Nie, X., Wang, P., Fu, X.D., Chen, C., et al. (2016). MicroRNA-21 lowers blood pressure in spontaneous hypertensive rats by upregulating mitochondrial translation. *Circulation* *134*, 734–751.
38. Moura, E., Pinto, C.E., Serrão, M.P., Afonso, J., and Vieira-Coelho, M.A. (2012). Adrenal α 2-adrenergic receptors in the aging normotensive and spontaneously hypertensive rat. *Neurobiol. Aging* *33*, 969–978.
39. Kintsurashvili, E., Gavras, I., Johns, C., and Gavras, H. (2001). Effects of antisense oligodeoxynucleotide targeting of the α (2B)-adrenergic receptor messenger RNA in the central nervous system. *Hypertension* *38*, 1075–1080.
40. Owens, E.A., Jie, L., Reyes, B.A.S., Van Bockstaele, E.J., and Osei-Owusu, P. (2017). Elastin insufficiency causes hypertension, structural defects and abnormal remodeling of renal vascular signaling. *Kidney Int.* *92*, 1100–1118.
41. Torella, D., Iaconetti, C., Catalucci, D., Ellison, G.M., Leone, A., Waring, C.D., Bochicchio, A., Vicinanza, C., Aquila, I., Curcio, A., et al. (2011). MicroRNA-133 controls vascular smooth muscle cell phenotypic switch in vitro and vascular remodeling in vivo. *Circ. Res.* *109*, 880–893.
42. Shan, Z., Qin, S., Li, W., Wu, W., Yang, J., Chu, M., Li, X., Huo, Y., Schaer, G.L., Wang, S., et al. (2015). An endocrine genetic signal between blood cells and vascular smooth muscle cells: role of microRNA-223 in smooth muscle function and atherogenesis. *J. Am. Coll. Cardiol.* *65*, 2526–2537.
43. Zhang, M.J., Yin, Y.W., Li, B.H., Liu, Y., Liao, S.Q., Gao, C.Y., Li, J.C., and Zhang, L.L. (2015). The role of TRPV1 in improving VSMC function and attenuating hypertension. *Prog. Biophys. Mol. Biol.* *117*, 212–216.
44. Yang, C.H., Yue, J., Fan, M., and Pfeffer, L.M. (2010). IFN induces miR-21 through a signal transducer and activator of transcription 3-dependent pathway as a suppressive negative feedback on IFN-induced apoptosis. *Cancer Res.* *70*, 8108–8116.
45. Degueurce, G., D'Errico, I., Pich, C., Ibberson, M., Schütz, F., Montagner, A., Sgandurra, M., Mury, L., Jafari, P., Boda, A., et al. (2016). Identification of a novel PPAR β /miR-21-3p axis in UV-induced skin inflammation. *EMBO Mol. Med.* *8*, 919–936.
46. van Rooij, E., and Olson, E.N. (2012). MicroRNA therapeutics for cardiovascular disease: opportunities and obstacles. *Nat. Rev. Drug Discov.* *11*, 860–872.
47. Melman, Y.F., Shah, R., Danielson, K., Xiao, J., Simonson, B., Barth, A., Chakir, K., Lewis, G.D., Lavender, Z., Truong, Q.A., et al. (2015). Circulating MicroRNA-30d is associated with response to cardiac resynchronization therapy in heart failure and regulates cardiomyocyte apoptosis: a translational pilot study. *Circulation* *131*, 2202–2216.
48. Hinkel, R., Penzkofer, D., Zühlke, S., Fischer, A., Husada, W., Xu, Q.F., Baloch, E., van Rooij, E., Zeiher, A.M., Kupatt, C., et al. (2013). Inhibition of microRNA-92a protects against ischemia/reperfusion injury in a large-animal model. *Circulation* *128*, 1066–1075.
49. van Rooij, E., Marshall, W.S., and Olson, E.N. (2008). Toward microRNA-based therapeutics for heart disease: the sense in antisense. *Circ. Res.* *103*, 919–928.
50. Xie, J., Ameres, S.L., Friedline, R., Hung, J.H., Zhang, Y., Xie, Q., Zhong, L., Su, Q., He, R., Li, M., et al. (2012). Long-term, efficient inhibition of microRNA function in mice using rAAV vectors. *Nat. Methods* *9*, 403–409.
51. Bylund, D.B., Eikenberg, D.C., Hieble, J.P., Langer, S.Z., Lefkowitz, R.J., Minneman, K.P., Molinoff, P.B., Ruffolo, R.R., Jr., and Trendelenburg, U. (1994). International Union of Pharmacology nomenclature of adrenoceptors. *Pharmacol. Rev.* *46*, 121–136.
52. Makaritsis, K.P., Johns, C., Gavras, I., and Gavras, H. (2000). Role of α (2)-adrenergic receptor subtypes in the acute hypertensive response to hypertonic saline infusion in anephric mice. *Hypertension* *35*, 609–613.
53. Kopp, U.C., Cicha, M.Z., and Smith, L.A. (2011). Impaired interaction between efferent and afferent renal nerve activity in SHR involves increased activation of α 2-adrenoceptors. *Hypertension* *57*, 640–647.
54. Shenouda, S.M., Johns, C., Kintsurashvili, E., Gavras, I., and Gavras, H. (2006). Long-term inhibition of the central α (2B)-adrenergic receptor gene via recombinant AAV-delivered antisense in hypertensive rats. *Am. J. Hypertens.* *19*, 1135–1143.
55. Owens, G.K., Kumar, M.S., and Wamhoff, B.R. (2004). Molecular regulation of vascular smooth muscle cell differentiation in development and disease. *Physiol. Rev.* *84*, 767–801.
56. Takwi, A.A., Li, Y., Becker Buscaglia, L.E., Zhang, J., Choudhury, S., Park, A.K., Liu, M., Young, K.H., Park, W.Y., Martin, R.C., et al. (2012). A statin-regulated microRNA represses human c-Myc expression and function. *EMBO Mol. Med.* *4*, 896–909.
57. Li, P., Yin, Y.L., Guo, T., Sun, X.Y., Ma, H., Zhu, M.L., Zhao, F.R., Xu, P., Chen, Y., Wan, G.R., et al. (2016). Inhibition of aberrant microRNA-133a expression in endothelial cells by statin prevents endothelial dysfunction by targeting GTP cyclohydrolase 1 in vivo. *Circulation* *134*, 1752–1765.
58. Galardi, S., Mercatelli, N., Farace, M.G., and Ciafrè, S.A. (2011). NF- κ B and c-Jun induce the expression of the oncogenic miR-221 and miR-222 in prostate carcinoma and glioblastoma cells. *Nucleic Acids Res.* *39*, 3892–3902.
59. Ma, F., Lin, F., Chen, C., Cheng, J., Zeldin, D.C., Wang, Y., and Wang, D.W. (2013). Indapamide lowers blood pressure by increasing production of epoxyeicosatrienoic acids in the kidney. *Mol. Pharmacol.* *84*, 286–295.
60. McDonald, O.G., Wamhoff, B.R., Hoofnagle, M.H., and Owens, G.K. (2006). Control of SRF binding to CarG box chromatin regulates smooth muscle gene expression in vivo. *J Clin Invest.* *116*, 36–48.
61. Bell, R.D., Deane, R., Chow, N., Long, X., Sagare, A., Singh, I., Streb, J.W., Guo, H., Rubio, A., Van Nostrand, W., et al. (2009). SRF and myocardin regulate LRP-mediated amyloid-beta clearance in brain vascular cells. *Nat Cell Biol.* *11*, 143–153.
62. Xiao, X., Li, J., and Samulski, R.J. (1998). Production of high-titer recombinant adeno-associated virus vectors in the absence of helper adenovirus. *J. Virol.* *72*, 2224–2232.
63. Zhang, F., Chen, C.L., Qian, J.Q., Yan, J.T., Cianflone, K., Xiao, X., and Wang, D.W. (2005). Long-term modifications of blood pressure in normotensive and spontaneously hypertensive rats by gene delivery of rAAV-mediated cytochrome P450 arachidonic acid hydroxylase. *Cell Res.* *15*, 717–724.

OMTN, Volume 11

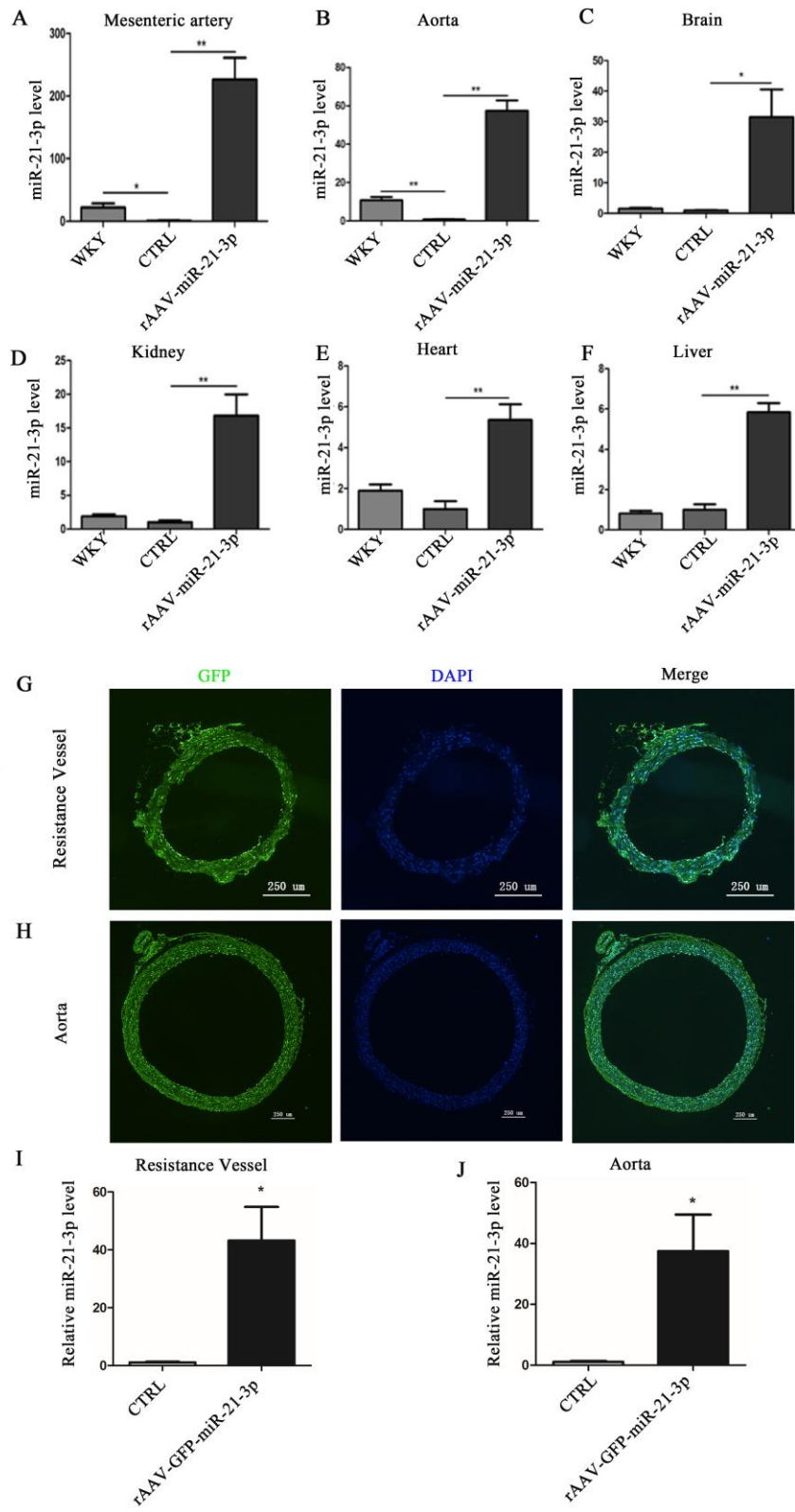
Supplemental Information

**Recombinant Adeno-Associated Virus-Mediated
Delivery of MicroRNA-21-3p Lowers Hypertension**

Feng Wang, Qin Fang, Chen Chen, Ling Zhou, Huaping Li, Zhongwei Yin, Yan Wang, Chun Xia Zhao, Xiao Xiao, and Dao Wen Wang

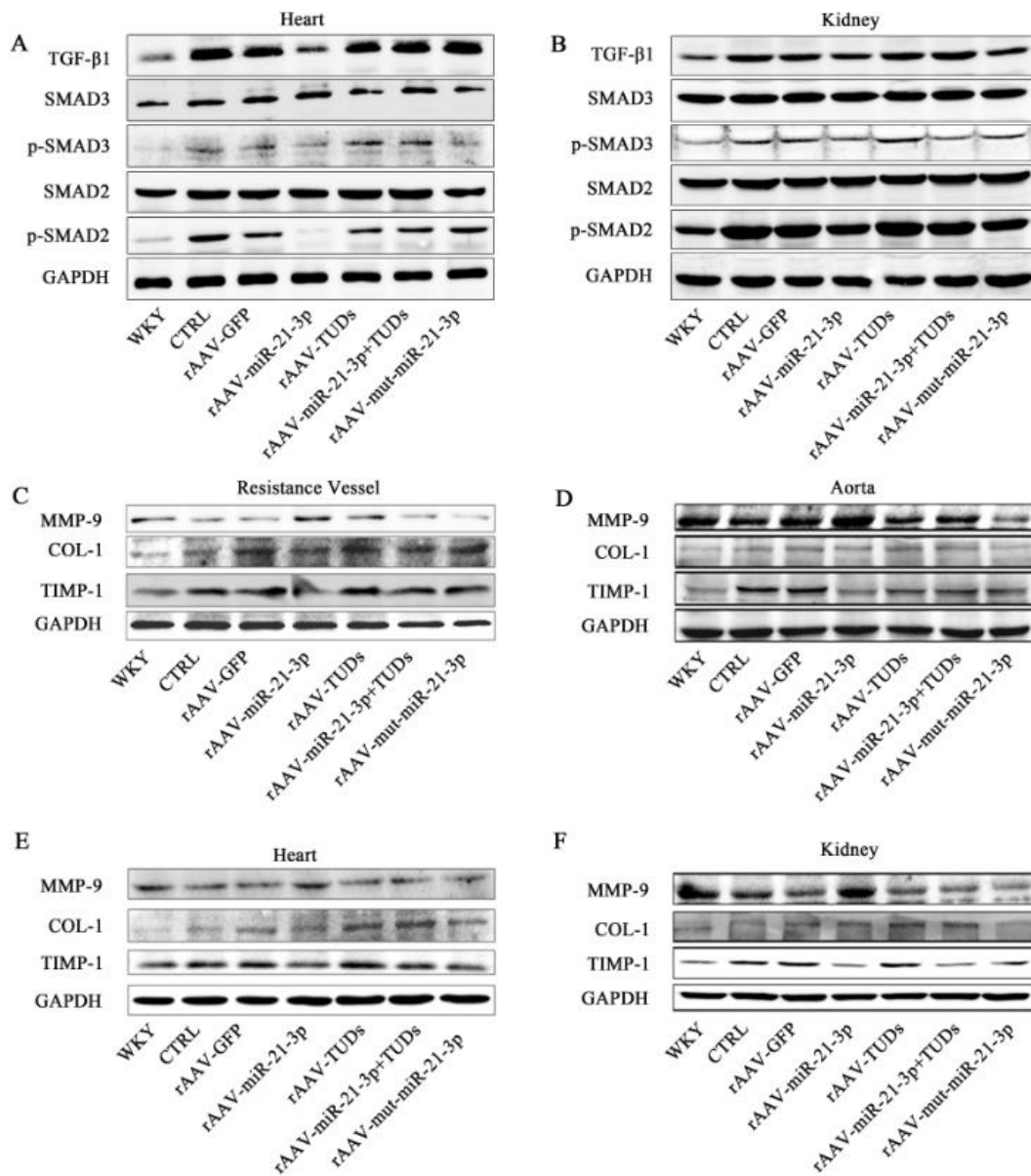
Supplemental Figure

Supplement Figure 1



Supplemental Figure 1. The expression of miR-21-3p in various tissues from WKYs, SHRs control and SHRs treated with rAAV-21-3p. (A-F) The levels of miR-21-3p in resistance vessel, aorta, brain, kidney, heart, and liver from WKYs, SHRs control and SHRs treated with rAAV-21-3p, respectively; (G-H) Immunofluorescence staining of GFP in resistance vessel and aorta from SHRs treated with rAAV-GFP-miR-21-3p, respectively (GFP, green; nuclei, blue); (I-J) The expression of miR-21-3p in resistance vessel and aorta from SHRs treated with rAAV-GFP-miR-21-3p, respectively. WKY, Wistar-Kyoto rat; CTRL, SHR-Control (treated with normal saline). Data are presented as mean \pm SEM ($n \geq 3$), * $p < 0.05$, ** $p < 0.01$.

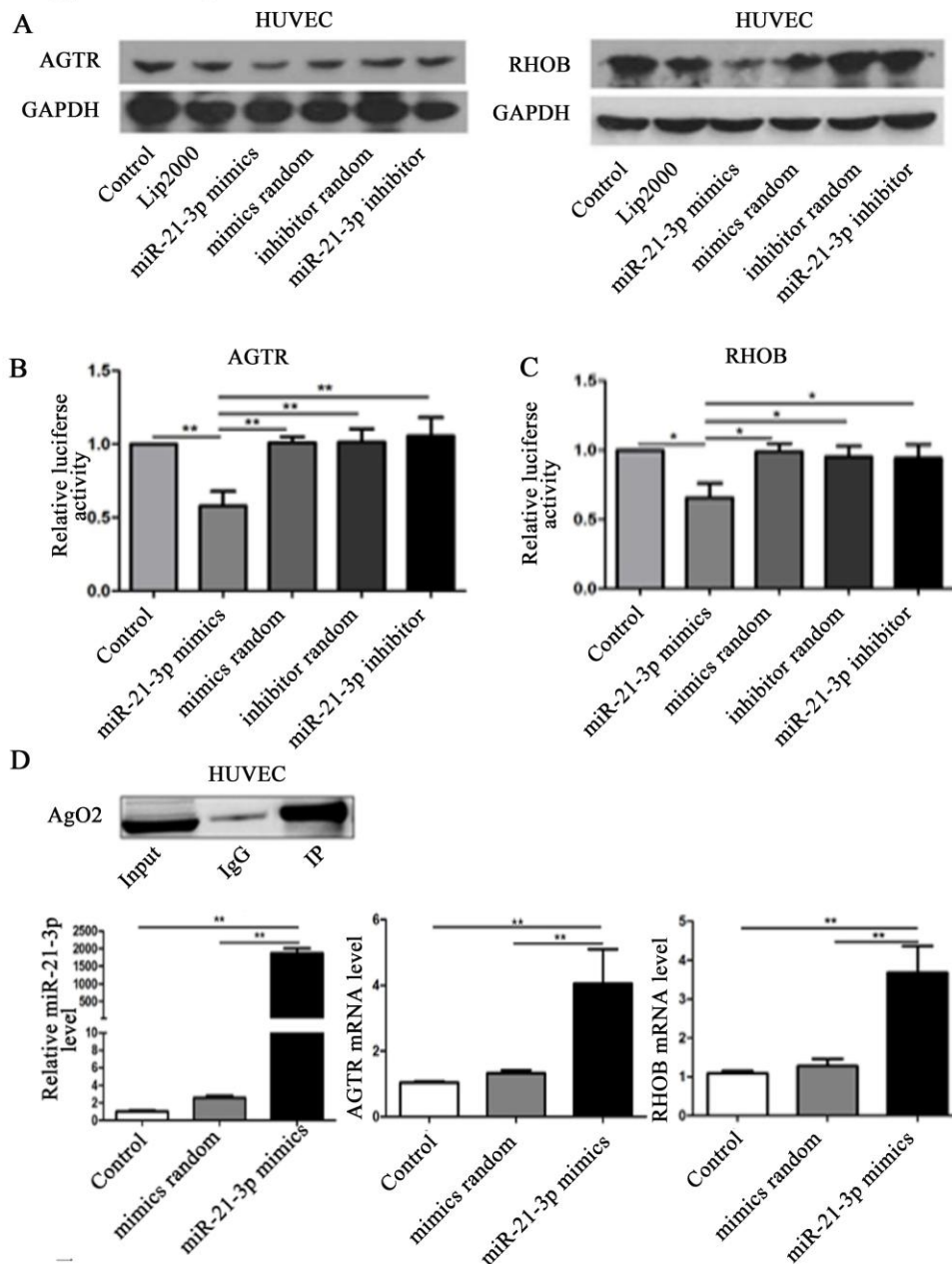
Supplemental Figure 2



Supplemental Figure 2. Influence of miR-21-3p on tissues fibrosis in SHRs. (A-B)

The protein expression of TGF- β 1, SMAD2, p-SMAD2, SMAD3 and p-SMAD3 in heart and Kidney from WKYs and SHRs with different treated; (C-F) The protein levels of TIMP1, MMP9, and COL1 in resistance vessels, aorta, heart and kidney from WKYs and SHRs with different treated. WKY, Wistar-Kyoto rat; CTRL, SHR-Control (treated with normal saline). Data are presented as mean \pm SEM ($n \geq 3$).

Supplement Figure 3



Supplemental Figure 3. miR-21-3p negatively regulates *AGTR1* and *RHOB* in

human. (A) The expression of *AGTR1* and *RHOB* proteins in HUVEC after treated

with miR-21-3p mimics; (B-C) The luciferase activity of pMIR-*AGTR1* 3'UTR and

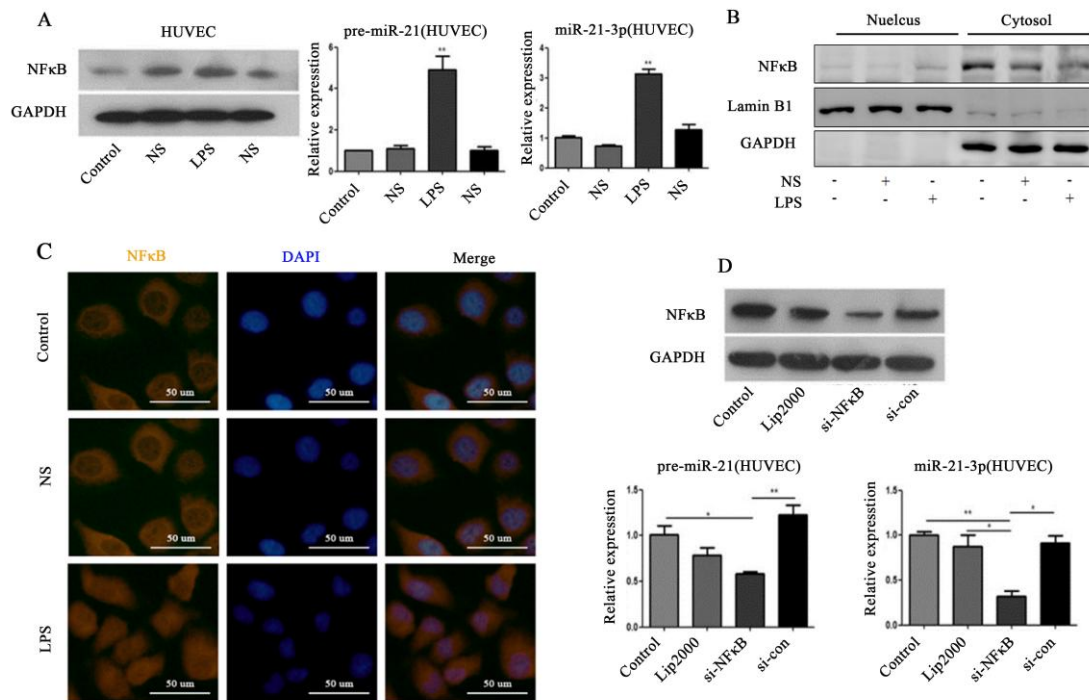
pMIR-*RHOB* 3'UTR plasmid in 239T cell after co-transfected with miR-21-3p

mimics; (D) The levels of *AGTR1* and *RHOB* mRNAs captured by

co-immunoprecipitation after administered with miR-21-3p mimics. lip2000,

lipofectamine 2000; Data are presented as mean \pm SEM (n \geq 3), *p<0.05, **p<0.01.

Supplement Figure 4



Supplemental Figure 4. NF-κB regulates the expression of miR-21-3p in HUVEC.

(A) The expressions of NF-κB p65 protein, precursor-miR-21, and mature miR-21-3p in HUVEC after stimulated by LPS; (B) The nuclear translocation of p65 in HUVEC after stimulated by LPS; (C) Immunofluorescence staining of HUVEC treated with or without LPS (NF-κB, red; nuclei, blue); (D) The expressions of NF-κB p65 protein, precursor-miR-21, and mature miR-21-3p in HUVEC after co-transfected with *NF-κB* siRNA. NS, saline; Lip2000, lipofectamine 2000; si-con, siRNA-negative control.

Data are presented as mean \pm SEM ($n \geq 3$), * $p < 0.05$, ** $p < 0.01$.

Supplemental Table 1. The baseline clinical characteristics of the hypertension patients

Characteristics	CTRL(n=32)	HYP1(n=33)	HYP2(n=15)	P value
Male/female (n/n)	22/9	15/18	7/8	0.089
Age (years)	53.0±11.1	56.9±9.6	59.6±9.9	0.102
BMI (kg/m ²)	23.4±2.4	23.8±2.2	23.2±2.8	0.785
SBP (mmHg)	120.1±1.8	149.7±2.7	123.9±1.7	<0.001
DBP (mmHg)	74.3±1.3	87.5±1.9	78.7±1.9	<0.001
Cr (mmol/L)	72.4±17.7	73.7±19.9	71.2±15.6	0.913
BUN (mmol/L)	5.5±1.3	6.0±1.2	6.3±2.6	0.224
Fasting glucose (mmol/L)	5.6±1.2	5.9±1.6	5.3±0.8	0.308
TG (mmol/L)	1.7±1.5	1.6±0.9	1.7±1.6	0.968
TC (mmol/L)	4.0±0.8	4.4±0.8	4.2±0.9	0.148
HDL (mmol/L)	1.1±0.3	1.1±0.2	1.2±0.3	0.351
LDL (mmol/L)	2.4±0.8	2.5±0.7	2.2±0.7	0.300

BMI, Body mass index; SBP, systolic blood pressure; DBP, diastolic blood pressure; Cr, Creatinine; BUN, Blood urea nitrogen; TG, Triglyceride; TC, total cholesterol; HDL, high-density lipoprotein; LDL, low-density lipoprotein; comparison among healthy control, hypertension patients with high blood pressure, and hypertension patients with normal blood pressure, Data are presented as mean \pm SEM.

Supplemental Table 2. The details of synthetic miR-21-3p expression sequences, miR-21-3p TuDs sequences, and mutated miR-21-3p expression sequences

	The sequence of synthetic sense
MiR-21-3p	5'-GATCCACAGCCCATCGACTGGTGTGTTCAAGAGACAACACCAGTCGATGGGCTGTCCGC-3'
MiR-21-3p TuDs	5'-GACGGCGCTAGGATCATCAACACAGCCCATCGATCTACTGGTGTGCAAGTATTCTGGTCACAGAATACAA CACAGCCCATCGATCTACTGGTGTGCAAGATGATCCTAGCGCCGTCTTTT-3'
Mutated miR-21-3p	5'-GATCCACAGCCCATCGACACCACAAGTTCAAGAGACTTGTGGTGTGCGATGGGCTGTCCGC-3'

Supplemental Table 3. Echocardiographic characteristics of WKYs and SHRs administered with various constructed virus

	WKY	CTRL	rAAV				
			GFP	miR-21-3p	TuDs	miR-21-3p + TuDs	mut-miR-21-3p
HR (b.p.m.)	449±18	451±26	458±17	466±9	453±8	449±39	456±15
LVPW,d (mm)	2.59±0.23	3.38±0.25	3.28±0.28	2.62±0.15 ^{#&}	3.70±0.15*	3.40±0.25*	3.51±0.11*
LVPW,s (mm)	3.44±0.27	4.54±0.33	4.42±0.25	3.85±0.18 ^{#&}	5.03±0.16*	4.48±0.16*	4.42±0.10*
LVAW,d (mm)	2.33±0.30	3.22±0.03	3.16±0.10	2.53±0.12 ^{#&}	3.25±0.17*	3.14±0.29*	3.10±0.13*
LVAW,s (mm)	3.12±0.38	4.29±0.11	4.23±0.25	3.59±0.15 ^{#&}	4.36±0.12*	4.21±0.09*	4.30±0.20*
LVID,d (mm)	4.38±0.20	4.86±0.23	4.97±0.22	4.95±0.27	4.51±0.24	4.75±0.15	4.68±0.45
LVID,s (mm)	2.08±0.06	3.29±0.29	3.22±0.25	2.18±0.21 ^{#&}	3.18±0.21*	3.13±0.43*	3.02±0.39*
FS (%)	74.6±1.25	53.8±2.85	58.2±4.16	65.2±1.48 ^{#&}	44.3±2.52*	54.7±1.67*	56.4±1.32*
EF (%)	81.9±0.19	60.1±0.23	61.0±3.78	75.1±1.67 ^{#&}	48.7±3.64*	59.6±6.93*	61.3±6.7*

Values represent mean ± SEM; n≥6 per group

HR, heart rate; LVPW,d, LV posterior wall thickness at diastole; LVPW,s, LV posterior wall thickness at systole; LVAW,d, LV anterior wall thickness at diastole; LVAW,s, LV anterior wall thickness at systole; LVID,d, LV internal diameter at diastole; LVID,s, LV internal diameter at

systole; FS, fractional shortening.

$p < 0.05$ VS. CTRL, SHR-Control (treated with normal saline); & $p < 0.05$ VS. rAAV-GFP; * $p < 0.05$ VS. rAAV-miR-21-3p.

Supplemental Table 4. Primers for amplification promoters of miR-21-3p

	Primer sequence
p1-Forward 1	5'- TTATGCCAAACGAATCCAGC-3'
p2-Forward 2	5'- GAATGTGATGTTTCAGCAGCAA-3'
p3-Forward 3	5'- GGAAAATCTGGTTGGTGTCTTAC-3'
Reverse	5'- GATGTCACGATGGTAGGCAAA-3'
	Primer sequence
f1-Forward 1	5'-CAAgCgATTCTCCTgCCTCA-3'
f2-Forward 2	5'-GTTATGCCAAACGAATCCAGC-3'
f3-Forward 3	5'-TCCTGCCCAACCCTTCCTC-3'
Reverse	5'-GGTCAGATGAAAGATACCAAAATGTC-3'

Supplemental Methods

Echocardiography analysis of WKYs and SHRs

At 24 weeks after rAAV delivery, WKYs and SHRs were anesthetized intraperitoneally with pentobarbital at a dose of 40 mg/kg body weight. Echocardiography was performed to assess the cardiac structure and functions of experimental rats using echocardiograph with VIVID 7 (General Electric, Milwaukee, WI), equipped with a 15-MHz linear array ultrasound transducer. The data of echocardiography was appropriately analyzed by 2 echocardiogram experts.

Prediction of miRNA Targets and Transcription factors

The microRNA databases and target prediction tools miRBase (<http://www.mirbase.org/>), miRanda (<http://www.microna.org/microna/home.do>), TargetScan (<http://www.targetscan.org/>), miRDB (<http://mirdb.org/miRDB/>) and RNAhybrid (<http://bibiserv.techfak.uni-bielefeld.de/rnahybrid/>) were used for predicting the potential targets of miR-21-3p. The transcription factors of miR-21-3p upstream were predicted via <http://www.gene-regulation.com/pub/programs.html>.

Cell Culture and Transfection

VSMCs, HUVEC and 293T cells were obtained from the American Type Tissue Collection, and were cultured in Dulbecco's modified Eagle's medium (DMEM, Gibco, Grand Island, NY) or Roswell Park Memorial Institute (RPMI) 1640 medium (RPMI 1640, Gibco, Grand Island, NY) supplemented with 10% fetal bovine serum (FBS, Gibco, Grand Island, NY), respectively. Cells were grown at 37 °C with an atmosphere of 5% CO₂. For the transfection of miRNAs, cells were treated with miR-21-3p mimics, mimics negative control, miR-21-3p inhibitors, and inhibitors

negative control at a final concentration of 100nM with lipofectamine 2000 (Invitrogen, Carlsbad, CA). 24-48 hours post-transfection, cells were harvested for RNA and protein, and functional assays were performed.

Plasmid Construction and Luciferase assay

The full length sequences of ADRA2B 3' UTR, AGTR1 3' UTR, and RHOB 3' UTR were amplified by PCR, then inserted into downstream of the luciferase reporter gene in the pMIR-REPORT™ Luciferase Vector (Promega, Madison, WI) and were termed as pMIR-ADRA2B-3'UTR, pMIR-AGTR1-3'UTR, and pMIR-BOHB-3'UTR, respectively. 200 ng of pMIR reporter plasmid containing the 3'UTR sequences of miR-21-3p targets and empty pMIR reporter plasmid along with renilla luciferase plasmid were cotransfected into 293 cells with 100 nM miR-21-3p mimics, mimics negative control by lipofectamine 2000, respectively.

The expression sequence of ADRA2B was designed and cloned into pcDNA3.1 expression vector (Invitrogen) according to the manufacturer's protocol (5'-GGTAT CCCC GACCT CCTA-3' and 5'-CCTGG CATAG ACAGC GAACA-3').

The expression sequence of SRF was designed and cloned into pcDNA3.1 expression vector (Invitrogen) according to the manufacturer's protocol (Human: 5'-CCCGTCCGCCCTCCTG-3' and 5'-TGAAAAGGCAACAATAAATAAGTGGT-3') (Rat: 5'-TTCCTCGCTGACTTGCCTGT-3' and 5'-CTGCCCACTCCTTCTCCCC-3')

By promoter deletion, several promoter segments of miR-21-3p transcript with different lengths were amplified by PCR (primers were recorded in Supplemental Table 4), then inserted into Basic pGL3 Luciferase Reporter Vector.

Cells were collected at 48 hours after transfection for detecting luciferase activity using Dual-Luciferase reporter assay system (Promega, Madison, WI). Firefly

luciferase activity was normalized to renilla luciferase activity. All experiments were performed in triplicate with data from three independent experiments.

RNA isolation and detection

Total RNA was isolated from plasma or frozen tissue samples by TRIzol LS or TRIzol Reagent (Invitrogen) according to the manufacturer's protocol, respectively. Two microgram of total RNA was reverse-transcribed using a reverse transcription kit (RevertAid M-MuLV RT, Thermo scientific). The Bulge-Loop™ miRNA qRT-PCR Detection Kit (Ribobio Co., Guangzhou, China) and Maxima SYBR Green/ROX qPCR Master Mix (Thermo scientific) were used for qRT-PCR to examine the relative quantification of miRNAs according to the manufacturer's protocol with the 7900HT Fast Real-Time PCR system (Applied Biosystems, Foster City). U6 was used as endogenous control for normalizing the data of qRT-PCR.

Western blot analysis

Western blots were performed as previously described¹.

RNA Immunoprecipitation

VSMCs and HUVEC were treated with miR-21-3p mimics and inhibitors for 48 hours using lipofectamine 2000, respectively. Lysed cell extracts were immunoprecipitated with anti-Ago2 antibody (Santa Cruz, CA) by protein G Sepharose beads as previously described². RNAs were extracted by Trizol LS reagent, and then miR-21-3p and its target mRNAs were detected by qRT-PCR after eluted from beads, respectively.

Functional experiments in superior mesenteric artery

Superior mesenteric arteries were carefully isolated and immersed in physiological salt solution (PSS) at 4 °C, containing (in mM) 119 NaCl, 4.7 KCl, 2.5 CaCl₂ H₂O, 1.17 MgSO₄ H₂O, 25 NaHCO₃, 1.18 KH₂PO₄, 0.027 EDTA, and 5.5 glucose, adjusted to pH 7.35-7.45. The bathing solution was gassed continuously with a mixture of 95% oxygen and 5% carbon dioxide at 37 °C. Isometric tension was measured using a force displacement transducer connected to a Mac Lab recording system (ADI Instruments, Australia). Small arterial rings (3mm in length) were suspended on 2 intraluminal parallel wires, and progressively stretched to an optimal basal tension of 1g. Bathing solution was replaced every 15min during a 60min equilibration period, if needed, the resting tension was readjusted to 1g.

At the beginning of the experiment, vessel rings were repeatedly stimulated with KCl solution (high K⁺, 60mM) for check their functional integrity. Subsequently, vessels were pre-contracted with norepinephrine (NE, 1nM-10uM) to stimulate vasoconstriction, and a cumulative relaxation responses to acetylcholine (Ach, 1nM-10uM) was performed to functionally evaluate the presence of endothelium. Thereafter, concentration-response curves to sodium nitroprusside (SNP 1nM-10uM) were recorded for determining the endothelium-independent vasodilatation.

Immunocytofluorescence

Cells and tissue sections were fixed in 4% paraformaldehyde for 10 min, and then soaked in 0.25% Triton-X100 for 10 min. After blocking with 5% BSA for 30 min, cells were incubated in primary antibody for 16h at 4°C, and then incubated with Cy3- or FITC conjugated secondary antibody for 2h at room temperature. Then, cells were visualized with DAPI (Boster) for nuclear staining.

References

1. Chen, F, Chen, C, Yang, S, Gong, W, Wang, Y, Cianflone, K, *et al.* (2012). Let-7b inhibits human cancer phenotype by targeting cytochrome P450 epoxygenase 2J2. *PloS one* **7**: e39197.
2. Goff, LA, Davila, J, Swerdel, MR, Moore, JC, Cohen, RI, Wu, H, *et al.* (2009). Ago2 immunoprecipitation identifies predicted microRNAs in human embryonic stem cells and neural precursors. *PLoS One* **4**: e7192.